Next-to-Leading order corrections to Deep Inelastic Scattering structure functions at small Bjorken-x

by

Henri Hänninen

Supervised by

Dr. Tuomas Lappi

Pro Gradu

University of Jyväskylä
Department of Physics

March 2017

Abstract

Experimentally determined Deep Inelastic Scattering structure functions have been successfully described at small Bjorken-x using the dipole picture of the scattering and leading order light cone perturbation theory. It is of interest whether this description can be bettered by studying higher order perturbation theory effects.

To improve the description, this work derives corrections to the Deep Inelastic Scattering cross sections and structure functions at next-to-leading order in light cone perturbation theory. To do this the framework of quantum field theory on the light cone is introduced along with necessities of perturbation theory on the light cone and the dipole picture of the scattering. The derived next-to-leading order cross section result has a soft divergence that is regulated with a cut-off, which then yields access to numerically evaluable cross sections and structure functions.

The next-to-leading order corrections are evaluated numerically and compared to established leading order results. It is found that while the regularization works, the divergence is over-subtracted leading to inviably large corrections to the leading result. This leads to the next-to-leading order cross section and structure function results becoming negative at high photon virtualities, which is unphysical. This result shows that a more careful approach to the regularization is needed.

Tiivistelmä

Syvän epäelastisen sironnan kokeellisia tuloksia on kuvattu onnistuneesti pienillä Bjorkenin x:n arvoilla käyttämällä sironnan dipolimallia ja johtavan kertaluvun valokartiohäiriöteoriaa. On tärkeää selvittää, paraneeko teorian kuvaavuus tutkimalla vaikutuksia korkeampien kertalukujen häiriöteoriasta.

Mittaustulosten kuvauksen parantamiseksi tässä työssä johdetaan korjauksia johtavan kertaluvun vaikutusalaan ja rakennefunktioihin häiriöteorian toisessa kertaluvussa. Tämän toteuttamiseksi esitellään tarvittavassa määrin valokartiokvanttikenttäteoria, pienen Bjorken-x sironnan dipolimalli ja häiriöteoriaa. Johdettu toisen kertaluvun vaikutusalala sisältää pehmeän divergenssin prosessin sisältämien sisäisten gluonien takia. Tämä divergenssi katkaisu-reguloidaan, mistä saadaan äärelliset numeerisesti laskettavat vaikutusalat ja rakennefunktiot.

Johdetut toisen kertaluvun korjaukset evaluoidaan numeerisesti ja verrataan tunnettuihin johtavan kertaluvun tuloksiin. Regularisaatio havaitaan toimivaksi, mutta katkaisu ei poista dirvergenssiä täysin ideaalisella tavalla, mikä johtaa kohtuuttoman suuriin toisen kertaluvun korjauksiin. Tämän seurauksena toisen kertaluvun vaikutusala ja rakennefunktio tuloksista tulee negatiivisia korkeilla fotonin virtualiteeteilla, mikä on epäfysikaalista. Tämä tulos kertoo, että regularisaatioon tarvitaan huolellisempi lähtestymistapa.

Contents

Chapter 1

Introduction

Ever since the discovery of the electron in the experiments by W. Crookes, A. Schuster, and J.J. Thomson in the late 19th century and the discovery of the proton by E. Rutherford in 1917, particle collision experiments have become an essential tool in particle and high energy physics. These experiments are an important cornerstone of modern physics as they make it possible to probe the fundamental dynamics of the elementary particles that constitute matter and radiation.

Important discoveries made in particle collision experiments in the last century include the discovery of the neutron in 1930s which led to the discovery of previously unknown fundamental forces, the weak force and the nuclear force, and the internal structure of nucleons. Driven by both theorists and experimentalists in the latter half of the 20th century a framework was developed that describes these particles and their interactions, nowadays known as the Standard Model. It has been incredibly successful in describing the strong, weak and electromagnetic forces along with successful predictions for the existence of particles such as the heavier bottom and top quarks found in 1977 and 1995, respectively, and the recently discovered Higgs Boson.

This Thesis is concerned with recent theoretical advancements in the understanding of a specific particle collision process called the Deep Inelastic Scattering (DIS). It is a relatively new process to study, being first tried in the 1960s and 1970s when it provided the first compelling evidence for the existence of quarks at the Standford Linear Accelerator Center (SLAC) in 1968. In Deep Inelastic

Scattering a high energy lepton, often an electron, is scattered of a hadronic target, e.g. a proton. "Deep" in the name refers to the high energy of the probing lepton – at high energy the de Broglie wavelength of the probe is smaller that the size of the target making it possible to resolve internal features of the hadron. "Inelastic" is in the name to specify that kinetic energy is transferred in the interaction, which would not happen in an elastic collision. Lastly, "scattering" is the general name for a physical process where a traveling particle is forced to deviate from its trajectory in a collision.

As a high energy process Deep Inelastic Scattering is well suited for the perturbative approach often used by theorists in particle physics. Commonly quantum chromodynamics (QCD) phenomena are studied perturbatively in the infinite momentum frame (IMF), which leads to the collinear factorization scheme and parton picture. However, Deep Inelastic Scattering can be studied in an alternative frame, the light cone frame, which leads to the dipole picture. The theory built in this framework is perturbative as well but it is structured in a different way than the perturbative QCD in the IMF. The DIS process has been calculated in leading order (LO) in this light cone perturbation theory [1] with quite successful description of the data from e.g. the Hadron-Electron Ring Accelerator (HERA) at the Deutsches Elektronen-Synchrotron (DESY).

We want to study the higher order perturbative effects to test the perturbation theory against experimental data. Additionally, consistency of the theory is desired so if a problem requires higher order perturbations for better description, it is good to cross check whether the extension to higher orders of the perturbation theory works for other problems. This leads us to study the next-to-leading order (NLO) corrections to the Deep Inelastic Scattering in the light cone perturbation theory, which is the topic of this Thesis.

In more technical terms the goal of this work is to compute next-to-leading order corrections to the quark dipole model [2] of Deep Inelastic Scattering at small Bjorken x, i.e. at very high collision energies. Due to the high energy scale the lepton-hadron scattering factorizes into an emission of a virtual photon by the lepton and an interaction between a virtual photon and the hadron, which at leading order occurs via the photon fluctuating into a quark-antiquark pair. At the next-to-leading order the process contains internal gluons and gluon loops in

addition to the quark dipole.

The body matter of this Thesis has the following structure. In Chapter 2 the Deep Inelastic Scattering, especially in the dipole picture, is introduced, along with select details about the perturbation theory that are necessary for the calculation. In Chapter 3 the theoretical calculations for the NLO corrections are carried out following [3], and the results are then studied numerically in Chapter 4.

Units and notation

The unit system used in this Thesis is the system of natural units commonly used in high energy physics. In this system the speed of light, reduced Planck's constant and Boltzmann constant are set to unity: $c = \hbar = k_B = 1$. This leads to the simplification of many relations between units and in fact is convenient to express mass, time, and length either in energy or reciprocal energy dimensions:

$$[\text{length}]^{-1} = [\text{time}]^{-1} = [\text{mass}] = [\text{energy}] = \text{GeV}.$$

When converting to and from SI units one then needs the relations:

$$1\,\text{eV} = 11600\,\text{K} = 1.60{\times}10^{-19}\,\text{J} = 5.07{\times}10^{6}\,\text{m}^{-1} = 1.52{\times}10^{15}\,\text{s}^{-1} = 1.78{\times}10^{-36}\,\text{kg},$$

or sometimes more conveniently

$$1\,\text{GeV} = 5.0677\,\text{fm}^{-1}.$$

Notation-wise, four-vectors will be denoted by plain characters, such as x for position. Two dimensional vectors will be used to describe quantities such as particle positions and momenta in the transverse plane with respect to the beam and they will be denoted by bold characters, such as $\mathbf{x}$.

Chapter 2

Deep Inelastic Scattering in dipole picture

An important physical process in experimental high energy physics is the Deep Inelastic Scattering. It enables testing of the theoretical approach of perturbative quantum chromodynamics through experiment and it yields a way to study the internal structure of hadrons through the parton distribution functions that can be found from the total lepton-hadron cross section. Deep inelastic scattering played a key part in the discovery quarks. Prior to the DIS experiments done at Stanford Linear Accelerator Center there was no substantial compelling experimental evidence for the reality of quarks and they were thought of as a mathematical tool by many.

In DIS a lepton scatters inelastically off a hadron or a nucleus breaking the target into other particles, depicted in Fig. 2.1. The interaction between the lepton and target is mediated by a virtual photon emitted by the lepton. Quantum Electrodynamics (QED) yields us a good understanding of this emission process and so the interesting and challenging part of DIS is the scattering of the virtual photon off the hadron or nucleus. Leptons are the probe of choice here due to the simplicity of the virtual photon emission from the lepton. The challenges in DIS arise from the virtual photon-hadron scattering due to the nature of the target. In a laboratory frame where the hadron, or the target nucleus composed of hadrons, has a large momentum the parton model applies and the target is

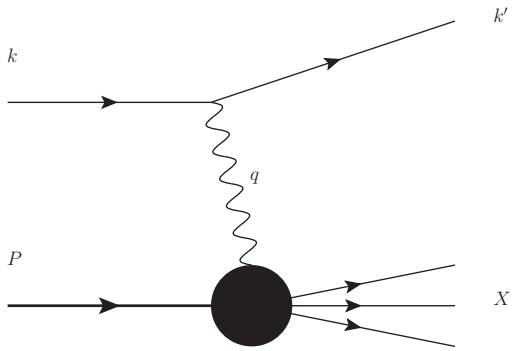

Figure 2.1: Schematic of the lepton-proton deep inelastic scattering. The scattering is mediated by a virtual photon.

composed of valence quarks, sea quarks, and gluons, whose dynamics are described by Quantum Chromodynamics (QCD), and hence is markedly more complex entity that the pointlike leptons. The frame in this picture of DIS is called the infinite momentum frame.

For a quantifiable discussion of the scattering we will need to define some Lorentz invariant kinematic variables. In the case of a proton target we set:

$$W^2 \coloneqq (P+q)^2 \tag{2.1}$$

$$Q^2 \coloneqq -q^2 = -(k-k')^2 \tag{2.2}$$

$$x \coloneqq \frac{Q^2}{2P\cdot q} = \frac{Q^2}{Q^2+W^2-m^2}. \tag{2.3}$$

Here, as shown in Fig. 2.1, P, k, k', q are the four-momenta of the target, incoming lepton, outgoing lepton and virtual photon, respectively. The variable W^2 describes the center of mass system total energy of the photon-proton scattering. In the case of the virtual photon that is off-shell, i.e. its four-momentum squared is non-zero, the amount it differs from zero is called its virtuality, denoted by Q^2. Lastly the third variable is the so-called Bjorken x. In the infinite momentum frame it corresponds to the fractional momentum carried the parton that the photon scatters from, with respect to the total momentum of the target.

In this work we will be studying DIS at small x in a regime where scattering off multiple partons is important, and the above parton picture is problematic. Additionally, since small x requires a large momentum from the photon, it can

be useful to describe the scattering in a frame that is traveling at the speed of light, where then the target has a small momentum. This calls for a suitable replacement for the parton picture, which is the dipole picture, and a formulation of the quantum field theory that works in such a frame.

2.1 DIS at small x: the Color Glass Condensate and the Dipole Picture

At small x in the infinite momentum frame at very high energies the target proton becomes highly Lorentz-contracted in the forward direction, i.e. a "pancake". In this kinematic regime the partons of the target have comparatively large-x and and as such become color sources by emitting soft, i.e. small-x, gluons, which go on emitting more soft gluons. This leads to a picture of the target where it consists essentially of high density small-x gluon matter. This is the Color Glass Condensate (CGC) model [4, 5] in which the hadronic matter is modeled as a semi-classical color field that consists of classical color sources radiating soft gluons [2].

Now let us study the scattering of a virtual photon from this CGC color field in the target proton's rest frame. Since the target is a color field that does not contain any electrical charge, the incoming virtual photon cannot see the target by itself. It turns out that in this regime the lifetime of a fluctuation of the photon into a quark-antiquark pair is significant in comparison to the target's size [2]. This leads to the dipole picture of DIS where in the dominating process the photon scatters from the color field by fluctuating into a quark-antiquark color dipole that interacts with the color field.

It is assumed that the quarks or the dipole scatter from the color field independently, during which the quark's transverse position can vary very little. The amount the position can change is $\Delta x_T \sim Rk_T/E$, where R is the longitudinal size of the target, k_T the change in transverse momentum obtained in the scattering, and E is the target rest frame energy of the quark dipole. One arrives at this approximation by considering the transverse distance Δx_T the quark travels over the longitudinal size of the target R after it is deflected by a small angle θ as it hits the target. This yields $\Delta x_T \sim \theta R$ and from kinematics one gets $\theta \sim k_T/E$,

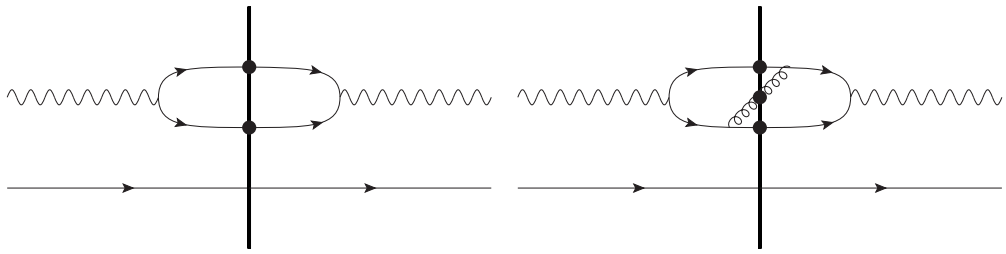

(a) LO **(b)** NLO

Figure 2.2: Simple schematics of the virtual photon-proton scattering. The second diagram shows one of the many possible NLO scattering processes.

yielding the above result. By calculating the Lorentz invariants (2.1) – (2.3) in the target rest frame, it is easy to see that at small x the energy of the dipole $E \sim 1/x$ is much larger than any other momentum scale in the problem. This means that at small x the transverse positions of the quarks are virtually unchanged, which justifies the approximation that the quark transverse position does not change in the scattering process. This is called the eikonal approximation and in other words it just assumes that the path of the quark through the color field is a straight line.

With the eikonal approximation the only effect the quarks undergo in the scattering off the color field is a color precession by a Wilson line [5], which will be quantified in Section 3.4. Lastly, after the dipole has scattered, it recombines into the end product of the scattering. The product considered here is a photon since we are calculating the cross section using the optical theorem which states that the total cross section of the photon-proton scattering is proportional to the forward elastic photon-proton scattering amplitude.

Since the path of the quark in the scattering process is a straight line, a convenient way to parametrize the problem is to use the longitudinal momenta and the positions of the particles in the transverse plane to describe the state. This will be called the mixed-space representation. We will see in Section 2.3 that our initial perturbation theory expansion will yield the incoming state wavefunction in momentum space and so we will need to concern ourselves with Fourier transforming the expansion result into this mixed space.

So, to summarize, at small x the deep inelastic scattering proceeds as follows. The lepton emits the virtual photon that then fluctuates into a quark-antiquark

pair. This color dipole then scatters elastically from the target and recombines into a photon. This leading order scattering is shown schematically in Fig. 2.2a and a contribution to the scattering process at next-to-leading order is shown in Fig. 2.2b.

The leading order result for the polarized cross section of this scattering is well known and has an especially handy form, for the virtual photon splitting process and the quark dipole scattering process factorize into their own terms [6]:

$$\sigma_{T,L}^{\gamma^*} = \sum_f \int d^2\mathbf{r} \int_0^1 dz \left|\Psi_{T,L}^{\gamma^* \to q\bar{q}}(\mathbf{x}, z, f)\right|^2 \sigma^{q\bar{q}}(\mathbf{r}), \tag{2.4}$$

where T and L denote the virtual photon's transverse and longitudinal polarizations, respectively. Here the first factor of the integrand is the squared wave function of the photon splitting, which describes the role of the splitting in the scattering in its entirety and the second factor is the so-called dipole cross section, describing the scattering the quark dipole from the target. Thus the photon splitting, a well understood QED process, and the complicated strong interaction factorize neatly. The convenience of this factorization is the fact that if one can solve for the dipole cross section, one can apply the result in other problems that factorize similarly. Proposed other applications of this factorization include diffractive structure functions [1], deeply virtual Compton scattering, and exclusive vector meson production [7].

The theoretical part of this thesis is essentially the derivation of a generalization of the leading order result (2.4) up to next-to-leading order in perturbation theory, following the method used in [3]. This goes roughly as follows: Taking the results of the Light Cone Quantum Field theory and perturbation theory, discussed in Sections 2.2 and 2.3, we can calculate the wavefunction of the splitting of the incoming photon up to next-to-leading order in perturbation theory. With this splitting wavefunction $\left|\gamma_{T,L}^*\right\rangle$ then we then can calculate the polarized cross sections roughly as $\sigma \sim \left\langle\gamma_{T,L}^*\right| 1 - \hat{S}_E \left|\gamma_{T,L}^*\right\rangle$ with the optical theorem and eikonal approximation which are discussed in quantified terms in Sections 2.3 and 3.4, respectively. In the numerical part of this work the calculated cross sections are evaluated and analyzed in Section 4.

2.2 Light Cone Quantum Chromodynamics

The perturbative QCD calculations of this work are carried out using the Light Cone Perturbation Theory (LCPT), where the Lorentz frame of the system is chosen to have velocity $v = 1$, as we can't do a Lorentz boost from a regular frame to get there. The properties of this formalism necessary for our calculations are introduced in this section. Much of this follows the comprehensive review article on the topic by S.J. Brodsky et al. [8], however a more pedagogical introduction to the topic can be found in the textbook [2].

Let $x = (x^0, x^1, x^2, x^3)$ be a 4-vector of the regular instant quantum field theory and $g_{\mu\nu}$ the standard Minkowski metric of special relativity

$$g_{\mu\nu} = \begin{pmatrix} 1 & 0 & 0 & 0 \\ 0 & -1 & 0 & 0 \\ 0 & 0 & -1 & 0 \\ 0 & 0 & 0 & -1 \end{pmatrix}. \tag{2.5}$$

The light cone 4-vector is then defined as $x = (x^+, x^1, x^2, x^-)$, where $x^+ := \frac{1}{\sqrt{2}}(x^0 + x^3)$ is called the light cone time and $x^- := \frac{1}{\sqrt{2}}(x^0 - x^3)$. The metric in the new frame becomes

$$g_{\mu\nu} = \begin{pmatrix} 0 & 0 & 0 & 1 \\ 0 & -1 & 0 & 0 \\ 0 & 0 & -1 & 0 \\ 1 & 0 & 0 & 0 \end{pmatrix}. \tag{2.6}$$

An inner product in these coordinates is then $x \cdot y := g_{\mu\nu} x^\mu y^\nu = x^+ y^- + x^- y^+ - x^1 y^1 - x^2 y^2$.

In this coordinate system a 4-momentum is $p = (p^+, p^1, p^2, p^-)$. The fourth component p^- is called the light cone energy as it contracts with the light cone time x^+ in the inner product and p^+ is the forward momentum. As we have $m^2 = p^2$, we can solve the light cone energy

$$p^- = \frac{m^2 + p_T^2}{2p^+} = \frac{p_T^2}{2p^+}, \tag{2.7}$$

where the second equality holds for massless particles and $p_T = (p^1, p^2)$ is the transverse momentum. Let us further define the fractional longitudinal momentum $z = \frac{k^+}{q^+}$ for our intermediate particles, where k^+ and q^+ are the light cone longitudinal momentum of the the intermediary particle and incoming photon respectively.

To quantize the field theory, we will need the parton Fock state creation and annihilation operators of the theory. They are $b^\dagger, b$ for quarks, $d^\dagger, d$ for anti-quarks, $a^\dagger, a$ for gluons and $a_\gamma^\dagger, a_\gamma$ for the photon. Their creation and annihilation operators commute or anti-commute in the following way:

$$\begin{aligned}&\Big\{b(\mathbf{x}', k'^+, h', A', f'), b^\dagger(\mathbf{x}, k^+, h, A, f)\Big\}\\ &= \Big\{d(\mathbf{x}', k'^+, h', A', f'), d^\dagger(\mathbf{x}, k^+, h, A, f)\Big\}\\ &= (2\pi)^3 2k^+\delta\Big(k^+ - k'^+\Big)\delta^{(2)}(\mathbf{x}-\mathbf{x}')\delta_{h,h'}\delta_{A,A'}\delta_{f,f'}\end{aligned} \tag{2.8}$$

$$\begin{aligned}&\Big[a(\mathbf{x}', k'^+, \lambda', a'), a^\dagger(\mathbf{x}, k^+, \lambda, a)\Big]\\ =&(2\pi)^3 2k^+\delta\Big(k^+ - k'^+\Big)\delta^{(2)}(\mathbf{x}-\mathbf{x}')\delta_{\lambda,\lambda'}\delta_{a,a'}.\end{aligned} \tag{2.9}$$

Here $\mathbf{x}$ is the transverse coordinate of the particle, k^+ forward light-cone momentum, h, λ helicities for fermions and photons respectively, f flavor and A, a the fundamental and adjoint color indices respectively. One gets these commutation relations from the similarly normalized momentum space relations with the Fourier transform relation:

$$b^\dagger\big(k^+, \mathbf{x}\big) = \int \frac{d^2\mathbf{k}}{2\pi} e^{-i\mathbf{k}\cdot\mathbf{x}} b^\dagger\big(k^+, \mathbf{k}\big), \tag{2.10}$$

which has the inverse transformation relation

$$b^\dagger\big(k^+, \mathbf{k}\big) = \int \frac{d^2\mathbf{x}}{2\pi} e^{i\mathbf{k}\cdot\mathbf{x}} b^\dagger\big(k^+, \mathbf{x}\big). \tag{2.11}$$

Antiquark and gluon operators have similar transformation relations as the quark creation operator $b^\dagger$ written out above. These Fourier transformations use the symmetric 1D normalization of $(2\pi)^{-1/2}$ which then in 2D yields the above normalization. With the above Fock state parton operators we can write the canonical

decompositions of the free fields for a fermion Ψ and a gauge field A:

$$\Psi_{\alpha Af}(x) = \sum_h \int \frac{dp^+ d^2p_T}{2p^+(2\pi)^3} \big(b(q,h,A,f) u_\alpha(p,h) e^{-ip\cdot x} + d^\dagger(q,h,A,f) v_\alpha(p,h) e^{+ip\cdot x} \big), \tag{2.12}$$

$$A^a_\mu(x) = \sum_\lambda \int \frac{dp^+ d^2p_T}{2p^+(2\pi)^3} \big(a(q,\lambda,a) \epsilon_\mu(p,\lambda) e^{-ip\cdot x} + a^\dagger(q,\lambda,a) \epsilon^*_\mu(p,\lambda) e^{+ip\cdot x} \big). \tag{2.13}$$

The normalization factor of the free fields above differs from the one used in [8] due to the choice of the anti-commutator normalization.

Lastly one needs the interaction terms of the light-cone Hamiltonian to calculate the vertex rules used in Sections 3.1 and 3.2. The QED interaction part of the Hamiltonian is [8]

$$P^-_{QED} = e \int dx^- d^2x_T \bar{\Psi} \not{A} \Psi + \frac{e^2}{2} \int dx^- d^2x_T \; \bar{\Psi} \gamma^+ \Psi \frac{1}{(i\partial^+)^2} \bar{\Psi} \gamma^+ \Psi \tag{2.14}$$

$$+ \frac{e^2}{2} \int dx^- d^2x_T \; \bar{\Psi} \not{A} \frac{\gamma^+}{i\partial^+} \not{A} \Psi, \tag{2.15}$$

where the Feynman slash notation $\not{A} \coloneqq A_\mu \gamma^\mu$ was used. Here the first term describes an interaction of the form $\gamma f \bar{f}$ and the latter two interactions of the type $f f \bar{f} \bar{f}$ and $f \bar{f} \gamma \gamma$. Out of these interaction types we will only need to be concerned with the first one which we will run into when the virtual photon splits into a quark and an antiquark.

For the QCD interaction term it is convenient to make the following definitions:

$$\begin{aligned} j^\nu_a(x) &\coloneqq \bar{\Psi} \gamma^\nu T^a \Psi, \\ \chi^\nu_a(x) &\coloneqq f^{abc} \partial^\nu A^\mu_b A^c_\mu, \\ J^\nu_a(x) &\coloneqq j^\nu_a(x) + \chi^\nu_a(x), \\ B^{\mu\nu}_a &\coloneqq f^{abc} A^\mu_b A^\nu_c, \end{aligned}$$

where T^a are the generators and f^{abc} are the structure constants of the $\mathfrak{su}(3)$ group. With these definitions the QCD interaction term of the Hamiltonian can

be written as [8]:

$$
\begin{aligned}
P^-_{QCD} &= g \int dx^- d^2x_T J^\mu_a A^a_\mu \\
&+ \frac{g^2}{4} \int dx^- d^2x_T \; B^{\mu\nu}_a B^a_{\mu\nu} \\
&+ \frac{g^2}{2} \int dx^- d^2x_T \; J^+_a \frac{1}{\left(i\partial^+\right)^2} J^+_a \\
&+ \frac{g^2}{2} \int dx^- d^2x_T \; \bar{\Psi}\gamma^\mu T^a A^a_\mu \frac{\gamma^+}{i\partial^+} \left(\gamma^\nu T^b A^b_\nu \Psi\right).
\end{aligned} \tag{2.16}
$$

Here the first term describes the interaction $gq\bar{q}$ which we will need for the vertex rule of the gluon emission which will take place in some of the possible next-to-leading order diagrams. The rest of the terms describe the gluon self-interactions ggg and $gggg$ along with multiple instantaneous fork interactions of the type $ggq\bar{q}$, which we will not need in this work. Here by fork interaction we are referring to the interactions where the parton number changes instantaneously by two, such as the ones shown in the Figs. 3.2c and 3.2d. For the vertex rule for these two interactions, we will need a mixed QED/QCD Hamiltonian term term that leads to the fork interaction $\gamma q\bar{q}g$ that is relevant in this scattering problem at next-to-leading order accuracy.

2.3 Perturbation theory on the light cone

In this section we present the necessities of perturbation theory on the light cone that we need to be able to calculate the cross sections. We will want to expand the wavefunction of the incoming photon in the Fock state basis for free on-shell partons at the instant of the collision with the target $x^+ = 0$. In order to describe the evolution of the state, we will need the full Hamiltonian on the light cone:

$$P^- = \mathcal{T} + P^-_{int} = \mathcal{T} + \mathcal{U}, \tag{2.17}$$

where $\mathcal{T}$ is the free part and the interaction part from above was renamed for convenience. In the interaction picture the light cone time evolution of operators is generated by $\mathcal{T}$; for the interaction operator $\mathcal{U}$ the time evolution can be written as

$$\mathcal{U}_I(x^+) = e^{i\mathcal{T}x^+}\mathcal{U}_I(0)e^{-i\mathcal{T}x^+}. \tag{2.18}$$

Then with this we can express the time evolution of a quantum state $|i_I\rangle$ from a time x_1 to x_2 with the time ordered exponential operator:

$$\left|i_I(x_2^+)\right\rangle = \mathcal{P}\exp\left(-i\int_{x_1^+}^{x_2^+} dx^+\mathcal{U}_I(x^+)\right)\left|i_I(x_1^+)\right\rangle. \tag{2.19}$$

We want to express this time evolution as an expansion in terms of a Fock state basis, that will be the parton Fock states. Our incoming virtual photon is an asymptotic state $\left|i_I(x_1^+ \to -\infty)\right\rangle$ and we want the scattering product state at collision instant to coincide with the Heisenberg picture: $\left|i_I(x_2^+ = 0)\right\rangle = |i_H\rangle$. To do the expansion we must first write out the time ordered exponential:

$$\begin{aligned}
&\mathcal{P}\exp\left(-i\int_{x_1^+}^{x_2^+} dx^+\mathcal{U}_I(x^+)\right) \\
&= \sum_{n=0}^{\infty}\frac{(-i)^n}{n!}\int_{x_0^+}^{x^+} dx_1^+dx_2^+\cdots dx_n^+\hat{\mathcal{T}}\left[\mathcal{U}_I(x_1^+)\cdots\mathcal{U}_I(x_n^+)\right] \\
&= \sum_{n=0}^{\infty}(-i)^n\int_{x_0^+}^{x^+} dx_1^+\int_{x_0^+}^{x_1^+} dx_2^+\cdots\int_{x_0^+}^{x_{n-1}^+} dx_n^+\mathcal{U}_I(x_1^+)\cdots\mathcal{U}_I(x_n^+),
\end{aligned} \tag{2.20}$$

where $\hat{\mathcal{T}}$ is the time ordering operator and the time ordering was undone at the second equality. Now plugging the expanded time ordered exponential (2.20) into the state evolution (2.19) and inserting the completeness relation of the Fock basis $\sum_{\mathcal{F}} |\mathcal{F}\rangle \langle\mathcal{F}| = \mathbf{1}$ before, after, and in between the interaction operators we get

$$|i_H\rangle = \left[\sum_{n=0}^{\infty}(-i)^n \sum_{\mathcal{F}_n}\cdots\sum_{\mathcal{F}_0}\int_{-\infty}^{0} dx_1^+ \int_{-\infty}^{x_1^+} dx_2^+ \cdots \int_{-\infty}^{x_{n-1}^+} dx_n^+ \, |\mathcal{F}_n\rangle \langle\mathcal{F}_n| \right. \tag{2.21}$$
$$\left. \mathcal{U}_I(x_1^+) \, |\mathcal{F}_{n-1}\rangle \langle\mathcal{F}_{n-1}| \cdots |\mathcal{F}_1\rangle \langle\mathcal{F}_1| \mathcal{U}_I(x_n^+) \, |\mathcal{F}_0\rangle \langle\mathcal{F}_0| \right] |i_I(-\infty)\rangle \, .$$

Now only thing remaining is to compute the nested integrals. However, these are not convergent as is in our asymptotic model and we must assume that the perturbation takes place adiabatically slowly:

$$\mathcal{U}_I(x_n^+) \to \mathcal{U}_I(x_n^+) e^{\epsilon x_n^+},$$

where $\epsilon > 0$.

Let us resolve these nested integrals by making a helpful iteration. First we look at the innermost integration of a term of order n, neglecting the summations over the basis for now:

$$\begin{aligned}
\int_{-\infty}^{x_{n-1}^+} dx_n^+ \, \langle\mathcal{F}_1| \mathcal{U}_I(x_n^+) \, |\mathcal{F}_0\rangle &= \int_{-\infty}^{x_{n-1}^+} dx_n^+ \, \langle\mathcal{F}_1| \, e^{i\mathcal{T}x_n^+} \mathcal{U}_I(0) e^{-i\mathcal{T}x_n^+} e^{\epsilon x_n^+} \, |\mathcal{F}_0\rangle \\
&= \langle\mathcal{F}_1| \mathcal{U}_I(0) \, |\mathcal{F}_0\rangle \int_{-\infty}^{x_{n-1}^+} dx_n^+ e^{i(\mathcal{T}_{\mathcal{F}_1} - \mathcal{T}_{\mathcal{F}_0} - i\epsilon)x_n^+} \\
&= \langle\mathcal{F}_1| \mathcal{U}_I(0) \, |\mathcal{F}_0\rangle \, \frac{1}{i(\mathcal{T}_{\mathcal{F}_1} - \mathcal{T}_{\mathcal{F}_0} - i\epsilon)} e^{i(\mathcal{T}_{\mathcal{F}_1} - \mathcal{T}_{\mathcal{F}_0} - i\epsilon)x_{n-1}^+},
\end{aligned} \tag{2.22}$$

where $\mathcal{T}_{\mathcal{F}_i}$ is the eigenvalue of $\mathcal{T}$ on $|\mathcal{F}_i\rangle$ and the integral converged at the lower limit thanks to the adiabatic weight. Plugging this back into (2.21) and repeating

this self-similar recursive integration process n times in the nth term one gets

$$
\begin{aligned}
|i_H\rangle &= \sum_{n=0}^{\infty}(-i)^n \sum_{\mathcal{F}_n}\cdots\sum_{\mathcal{F}_0} |\mathcal{F}_n\rangle \frac{1}{i(\mathcal{T}_{\mathcal{F}_n}-\mathcal{T}_{\mathcal{F}_0}-i\epsilon)} \langle\mathcal{F}_n|\,\mathcal{U}_I(0)\,|\mathcal{F}_{n-1}\rangle \\
&\quad \times\cdots\times \frac{1}{i(\mathcal{T}_{\mathcal{F}_1}-\mathcal{T}_{\mathcal{F}_0}-i\epsilon)} \langle\mathcal{F}_1|\,\mathcal{U}_I(0)\,|\mathcal{F}_0\rangle \langle\mathcal{F}_0|i_I(-\infty)\rangle \\
&= \sum_{\mathcal{F}_0}\langle\mathcal{F}_0|i_I(-\infty)\rangle \Bigg[|\mathcal{F}_0\rangle + \sum_{n=1}^{\infty}\sum_{\mathcal{F}_n}\cdots\sum_{\mathcal{F}_1} |\mathcal{F}_n\rangle \frac{1}{(\mathcal{T}_{\mathcal{F}_0}-\mathcal{T}_{\mathcal{F}_n}+i\epsilon)} \\
&\quad \langle\mathcal{F}_n|\,\mathcal{U}_I(0)\,|\mathcal{F}_{n-1}\rangle \frac{1}{(\mathcal{T}_{\mathcal{F}_0}-\mathcal{T}_{\mathcal{F}_{n-1}}+i\epsilon)} \langle\mathcal{F}_{n-1}|\,\mathcal{U}_I(0)\,|\mathcal{F}_{n-2}\rangle \\
&\quad \times\cdots\times \langle\mathcal{F}_2|\,\mathcal{U}_I(0)\,|\mathcal{F}_1\rangle \frac{1}{(\mathcal{T}_{\mathcal{F}_0}-\mathcal{T}_{\mathcal{F}_1}+i\epsilon)} \langle\mathcal{F}_1|\,\mathcal{U}_I(0)\,|\mathcal{F}_0\rangle \Bigg],
\end{aligned}
\tag{2.23}
$$

which finally is the result we can use.

The Fock basis used here is in momentum-space where $\mathcal{T}$ is diagonal, which it would not be in the mixed-space where we would like to represent the scattering amplitudes for the calculation of the cross sections. Therefore for our use case we must Fourier transform the momentum-space parton operators into mixed-space representation via the relation (2.11).

Once the perturbative state is known in mixed space one gets the scattering cross section by optical theorem

$$
\sigma^{\gamma}_{T,L}[\mathcal{A}] = \frac{1}{2\pi q^+\delta(q'^+-q^+)}\,\mathrm{Re}\left({}_{NLO}\langle\gamma^*_{T,L}|\,1-\hat{S}_E\,|\gamma^*_{T,L}\rangle_{NLO}\right), \tag{2.24}
$$

where $\hat{S}_E$ is the eikonal scattering operator [3].

Chapter 3

From photon splitting amplitudes to computable cross sections

The general structure of the theoretical calculations done in this chapter consist of three main parts. First we start from the perturbation theory discussed in Section 2.3 and calculate the splitting amplitude of the virtual photon in leading and next-to-leading order, which is done in Sections 3.1 and 3.2, respectively. To do this one starts by writing the momentum-space Fock basis expansion (2.23) for the virtual photon to either LO or NLO and then Fourier transforming this into mixed-space. With these wavefunctions one can then calculate the cross sections which is done in Section 3.4. Lastly, the cross sections will have divergences which are regulated in Section 3.5. This chapter follows the work done in [3].

3.1 Virtual photon splitting at leading order

Let us first briefly go through the leading order perturbation theory calculation to get a grasp on the procedure. In the leading order there is only one diagram relevant to the process, shown in Fig. 3.1.

At the leading order of the perturbative expansion (2.23) the photon splitting amplitude is

$$|\gamma^*\rangle_{LO} = \sum_{q\bar{q}\ states} \frac{\langle q\bar{q}|\,\hat{\mathcal{U}_I}(0)\,|\gamma^*\rangle}{\Delta k^-}\,|q\bar{q}\rangle\,, \tag{3.1}$$

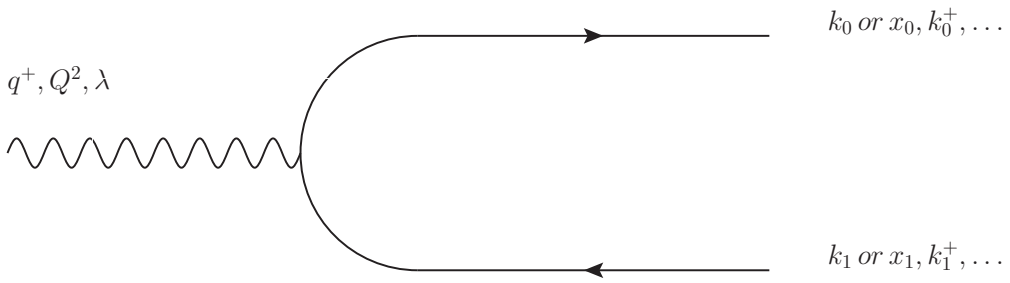

Figure 3.1: The leading order diagram for the photon splitting into the quark-antiquark dipole.

where $\hat{\mathcal{U}}$ is the interaction operator of the theory, Δk^- is the difference in light cone energy between the initial and final states, and the sum is taken to be over all the possible quark-antiquark configurations. To calculate this, we need the the vertex rules for the photon splitting, that are derived from the QED interaction Hamiltonian (2.14) discussed in Section 2.2. This derivation of the vertex rules has been done in [3] and is a bit more involved than in covariant quantum field theory where the leptonic tensor factorizes out straightforwardly. This is because in the light cone formalism there are no virtual particles or longitudinally polarized photons.

First, let the incoming photon have longitudinal momentum q^+, virtuality Q^2 and polarization λ and the final state quark and antiquark have the indices 0 and 1 respectively, so that the annihilation and creation operators have the following arguments:

$$\begin{aligned} a_\gamma &:= a_\gamma(q^+, Q^2, \lambda) \\ b &:= b(k_0^+, \mathbf{k_0}, h_0, A_0, f) \\ d &:= d(k_1^+, \mathbf{k_1}, h_1, A_1, f), \end{aligned}$$

where h_i are the helicities, A_i the colors and f the flavor of the particles. Furthermore, let us denote the interaction operator of the theory at $x^+ = 0$ by $\hat{V} := \hat{U}_I(0)$.

The vertex rules, derived in [3], for the photon splitting to a quark and an antiquark depend on the polarization of the photon – for the transversely polarized

photon we have:

$$\langle 0|\, db\hat{V} a_\gamma^\dagger \,|0\rangle = (2\pi)^3 \delta\big(k_0^+ + k_1^+ - q^+\big)\delta(\mathbf{k}_0 + \mathbf{k}_1 - \mathbf{q}) e e_{f_0} \delta_{f_0,f_1}\delta_{A_0,A_1}\delta_{h_0,-h_1} \\ \times \sqrt{4k_0^+ k_1^+}\,\epsilon_\lambda \cdot \left[\frac{\mathbf{q}}{q^+} - \left(\frac{1+2h_0\lambda}{2}\right)\frac{\mathbf{k}_1}{k_1^+} - \left(\frac{1-2h_0\lambda}{2}\right)\frac{\mathbf{k}_0}{k_0^+}\right], \tag{3.2}$$

and for the longitudinal photon we have an effective vertex rule:

$$\langle 0|\, db\hat{V} a_\gamma^\dagger \,|0\rangle = (2\pi)^3 \delta\big(k_0^+ + k_1^+ - q^+\big)\delta(\mathbf{k}_0 + \mathbf{k}_1 - \mathbf{q}) e e_{f_0} \delta_{f_0,f_1}\delta_{A_0,A_1}\delta_{h_0,-h_1} \\ \times \sqrt{4k_0^+ k_1^+}\,\frac{Q}{q^+}, \tag{3.3}$$

where in addition to the longitudinal and transverse momenta we have the parameters f for quark flavor, A for color and h for helicity.

In the light cone formalism the dipole production can happen via two distinct routes: either the lepton emits a transverse photon which then fluctuates into the quark dipole or the dipole is produced in an instantaneous lepton to lepton, quark and antiquark interaction where the leptonic and quark currents Coulomb interact directly. The former process is obviously associated with the former vertex rule above whereas the latter is interpreted to be mediated by a longitudinal photon, yielding the latter effective vertex rule. This is discussed in better detail in [3].

Lastly, we need to understand what is actually meant by the sum over the final states: each quark has some transverse and longitudinal momenta, in addition to the relevant discrete quantum numbers: helicity, color and flavor. This means that the sum over end states implies integrations over the momenta with appropriate normalization and sums over the quantum numbers, i.e.

$$\sum_{q\bar{q}\ states} \rightsquigarrow \sum_{h_0,A_0,f_0}\sum_{h_1,A_1,f_1}\int \frac{dk_0^+}{2\pi 2k_0^+}\int\frac{d^2\mathbf{k}_0}{(2\pi)^2}\int\frac{dk_1^+}{2\pi 2k_1^+}\int\frac{d^2\mathbf{k}_1}{(2\pi)^2}. \tag{3.4}$$

With the above considerations we can write out the splitting amplitude (3.1),

which becomes for the transverse polarization:

$$
\begin{aligned}
\left|\gamma_T^*(q^+,Q^2)\right\rangle_{LO} = & \sum_{h_0,A_0,f_0}\sum_{h_1,A_1,f_1}\int\frac{dk_0^+}{2\pi 2k_0^+}\int\frac{d^2\mathbf{k}_0}{(2\pi)^2}\int\frac{dk_1^+}{2\pi 2k_1^+}\int\frac{d^2\mathbf{k}_1}{(2\pi)^2} \\
& \times (2\pi)^3\delta\big(k_0^+ + k_1^+ - q^+\big)\delta(\mathbf{k}_0+\mathbf{k}_1-\mathbf{q})ee_{f_0}\delta_{f_0,f_1}\delta_{A_0,A_1}\delta_{h_0,-h_1} \\
& \times \sqrt{4k_0^+k_1^+}\epsilon_\lambda\cdot\left[\frac{\mathbf{q}}{q^+}-\left(\frac{1+2h_0\lambda}{2}\right)\frac{\mathbf{k}_1}{k_1^+}-\left(\frac{1-2h_0\lambda}{2}\right)\frac{\mathbf{k}_0}{k_0^+}\right] \\
& \times \frac{1}{\Delta k^-}b^\dagger(k_0^+,..)d^\dagger(k_1^+,..)\left|0\right\rangle \\
= & \frac{e}{2\cdot 2\pi}\int\frac{dz_0}{\sqrt{z_0}}\int\frac{dz_1}{\sqrt{z_1}}\delta(z_0+z_1-1)\int\frac{d^2\mathbf{k}_0}{(2\pi)^2}\sum_{h_0}\left[z_1-z_0-2h_0\lambda\right] \\
& \times \frac{\epsilon_\lambda\cdot\mathbf{k}_0}{z_0z_1Q^2+\mathbf{k}_0^2}\times\sum_{f_0}e_{f_0}\sum_{A_0}b^\dagger(k_0^+,..)d^\dagger(k_1^+,..)\left|0\right\rangle,
\end{aligned}
\tag{3.5}
$$

where we needed the following relations stemming from the kinematics of the system, $\mathbf{q}=0$:

$$
\Delta k^- = -\frac{Q^2}{2q^+}-k_0^- - k_1^- = -\frac{1}{2q^+z_0z_1}\big(z_0z_1Q^2+\mathbf{k}_0^2\big)
$$

and

$$
\left[\frac{\mathbf{q}}{q^+}-\left(\frac{1+2h_0\lambda}{2}\right)\frac{\mathbf{k}_1}{k_1^+}-\left(\frac{1-2h_0\lambda}{2}\right)\frac{\mathbf{k}_0}{k_0^+}\right] = \frac{\mathbf{k}_0}{2q^+z_0z_1}[z_0-z_1+2h_0\lambda].
$$

In a similar vein we get for the longitudinal photon splitting the amplitude

$$
\begin{aligned}
\left|\gamma_L^*\right\rangle_{LO} = & -\frac{e}{2\pi}\int\frac{dz_0}{\sqrt{z_0}}\int\frac{dz_1}{\sqrt{z_1}}\delta(z_0+z_1-1)\int\frac{d^2\mathbf{k}_0}{(2\pi)^2} \\
& \times\frac{z_0z_1Q^2}{z_0z_1Q^2+\mathbf{k}_0^2}\times\sum_{f_0}e_{f_0}\sum_{h_0,A_0}b^\dagger(k_0^+,..)d^\dagger(k_1^+,..)\left|0\right\rangle.
\end{aligned}
\tag{3.6}
$$

We need the amplitude in the mixed-space of particle positions and fractional momenta in order to apply the eikonal approximation, so next the above amplitudes must the Fourier transformed from momentum-space into the mixed-space. For

this we need the operator Fourier transformation relation (2.11) and two integration formulae that can be found in [3]:

$$\int \frac{d^2\mathbf{k}}{2\pi}\frac{e^{i\mathbf{k}\cdot\mathbf{x}}}{Q^2+\mathbf{k}^2}\mathbf{k}^\mu = i\frac{\mathbf{x}^\mu}{|\mathbf{x}|}QK_1(Q|\mathbf{x}|) \tag{3.7}$$

$$\int \frac{d^2\mathbf{k}}{2\pi}\frac{e^{i\mathbf{k}\cdot\mathbf{x}}}{Q^2+\mathbf{k}^2} = K_0(Q|\mathbf{x}|), \tag{3.8}$$

where $K_0(x)$ and $K_1(x)$ are modified Bessel functions of the second kind. Carrying out the Fourier transform the wavefunctions of either polarization of the photon get a shared structure:

$$\begin{aligned}\mathcal{F}\left|\gamma^*_{T,L}\right\rangle_{LO} = \frac{e}{2}\int\int\frac{dz_0}{\sqrt{z_0}}\frac{dz_1}{\sqrt{z_1}}\delta(z_0+z_1-1)\int\int\frac{d^2\mathbf{x}_0}{(2\pi)^2}\frac{d^2\mathbf{x}_1}{(2\pi)^2}\\ \times\sum_{h_0}\Phi^{LO}_{T,L}(Q^2,\mathbf{x}_0,\mathbf{x}_1,z_0,z_1,(h_0,\lambda)\sum_f e_f\times\sum_{A_0}b^\dagger(k_0^+,..)d^\dagger(k_1^+,..)\left|0\right\rangle,\end{aligned} \tag{3.9}$$

where the polarization dependent factors are

$$\Phi^{LO}_T(Q^2,\mathbf{x}_0,\mathbf{x}_1,z_0,z_1,h_0,\lambda) = i[z_1-z_0-2h_0\lambda]\frac{\epsilon_\lambda\cdot\mathbf{x}_{01}}{|\mathbf{x}_{01}|^2}\cdot Q\sqrt{z_0z_1\mathbf{x}_{01}^2}K_1\left(Q\sqrt{z_0z_1\mathbf{x}_{01}^2}\right) \tag{3.10}$$

$$\Phi^{LO}_L(Q^2,\mathbf{x}_0,\mathbf{x}_1,z_0,z_1) = -2z_0z_1QK_0\left(Q\sqrt{z_0z_1\mathbf{x}_{01}^2}\right). \tag{3.11}$$

The result for the splitting wavefunction (3.9), along with (3.10) and (3.11), match the results calculated in [9] when one neglects the quark masses and takes into account the different normalization and notation.

It turns out in Section 3.4 that in order to calculate the photon cross sections, we will need the above factors, (3.10) and (3.11), squared and summed over the relevant set of quantum numbers, which is the helicity of the quark h_0 in the longitudinal case and the helicity and the photon polarization λ in the transverse case. The so-called impact factors are defined as

$$\mathcal{I}^{LO}_L(Q^2,\mathbf{x}_0,\mathbf{x}_1,z_0,z_1) \coloneqq \frac{1}{2}\sum_{h_0}\left|\Phi^{LO}_L(Q^2,\mathbf{x}_0,\mathbf{x}_1,z_0,z_1)\right|^2 \tag{3.12}$$

$$\mathcal{I}_T^{LO}(Q^2, \mathbf{x}_0, \mathbf{x}_1, z_0, z_1) \coloneqq \frac{1}{4}\sum_{h_0,\lambda} \left|\Phi_T^{LO}(Q^2, \mathbf{x}_0, \mathbf{x}_1, z_0, z_1, h_0, \lambda)\right|^2, \tag{3.13}$$

where the prefactors contain an additional factor of $1/2$ by convention, as in [3], in addition to the $1/2$ in the transverse case arising from the averaging over the photon polarizations $\lambda = \pm 1$. Applying the impact factors with this convention at the cross section phase then includes a corresponding scaling by two. As the splitting amplitude of the longitudinally polarized photon is independent of the quark helicity the impact factor simply becomes

$$\mathcal{I}_L^{LO}(Q^2, \mathbf{x}_0, \mathbf{x}_1, z_0, z_1) = 4z_0 z_1 Q^2 K_0(Q\sqrt{z_0 z_1 \mathbf{x}_{01}})^2. \tag{3.14}$$

For the transverse polarization of the photon the functional structure of the cross section will turn out to be more complex and we'll need to know that the polarization vector ϵ_λ satisfies a relation

$$\sum_{\lambda\in\{-1,1\}} \epsilon_\lambda^{i*}\epsilon_\lambda^{j} = \delta^{ij}, \tag{3.15}$$

with which we can compute that

$$\sum_{h_0,\lambda} [z_1 - z_0 - 2h_0\lambda]^2 (\epsilon_\lambda^* \cdot \mathbf{x}_{01})(\epsilon_\lambda \cdot \mathbf{x}_{01}) = 4\big(z_0^2 + z_1^2\big)\mathbf{x}_{01}^2,$$

which yields us the result

$$\mathcal{I}_T^{LO}(Q^2, \mathbf{x}_0, \mathbf{x}_1, z_0, z_1) = \big(z_0^2 + z_1^2\big) z_0 z_1 Q^2 K_1(Q\sqrt{z_0 z_1 \mathbf{x}_{01}})^2. \tag{3.16}$$

The results (3.14) and (3.16) will be needed in the Section 3.4 where we will calculate the cross section of the photon-color field scattering.

Above we saw the outline how the photon splitting amplitude is calculated in the leading order using light cone quantum field theory. In the next section we will head right into the main work of this thesis, where we will go through the calculation in next-to-leading order accuracy.

3.2 Virtual photon splitting at next-to-leading order

In this section the next-to-leading order wavefunction of the virtual photon fluctuating into a quark-antiquark-gluon state is calculated. This is carried out by starting from the second order in the perturbative expansion (2.23) and calculating the NLO wavefunction for the quark-antiquark-gluon $q\bar{q}g$ production which is then Fourier transformed into mixed space.

The $q\bar{q}g$ production from the initial virtual photon can take place via four different processes, shown in Fig. 3.2. Just like in LO, both a transverse and longitudinal photon can first decay into the quark-antiquark pair in a QED process and then either one of the quarks then emits the gluon. Alternatively, the transverse photon can decay in an instantaneous QED/QCD process straight into the $q\bar{q}g$ triplet. The former case then has the intermediate state of a quark and an antiquark whereas the latter does not.

Similarly to the LO case, let the incoming photon have longitudinal momentum q^+, virtuality Q^2 and polarization λ and the final state quark, antiquark, and gluon have the indices 0, 1, and 2, respectively, so that the annihilation and creation operators have the following arguments:

$$\begin{aligned} a_\gamma &:= a_\gamma(q^+, Q^2, \lambda) \\ b &:= b(k_0^+, \mathbf{k_0}, h_0, A_0, f) \\ d &:= d(k_1^+, \mathbf{k_1}, h_1, A_1, f) \\ a &:= a(k_2^+, \mathbf{k_2}, \lambda_2, a), \end{aligned} \tag{3.17}$$

where h_i are the helicities, A_i, a the colors and f the flavor of the particles. Additionally for the states that have an intermediate quark or antiquark, we will give the intermediate particle's arguments the indices i and j, for a quark and an antiquark respectively, to differentiate them from their final state counterparts. Lastly denote the interaction operator of the theory at $x^+ = 0$ by $\hat{V} := \hat{U}_I(0)$. Then by writing out the perturbative expansion (2.23) up to the second order the

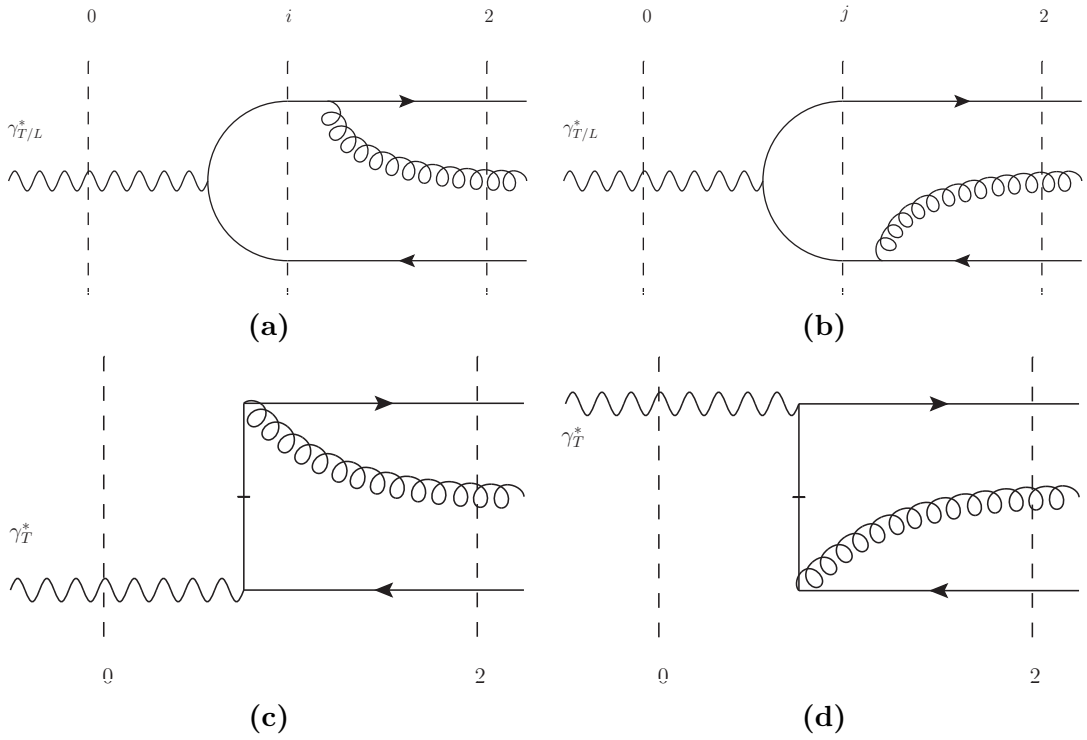

Figure 3.2: The four possible real process diagrams to be considered in the next-to-leading order calculation. In figures (a) and (b) the virtual photon first splits in a QED process into the quark-antiquark pair after which either of the quarks emits a gluon. In figures (c) and (d) the quark-anti-quark-gluon end state is reached at once in an instantaneous QED/QCD process. The diagrams are ordered horizontally in light cone time x^+, the initial state $x^+ = -\infty$ being on the left edge of each diagram and the interaction instant $x^+ = 0$ being on the right. The dashed lines denote Fock states in the diagrams relevant for the calculation. Initial and final states are denoted by 0 and 2, respectively, and in figures (a) and (b) the intermediate states before the gluon emission are denoted by i and j for the quark and antiquark emission cases, respectively.

wavefunction of the splitting can then be written as

$$\begin{aligned}\left|\gamma^*(q^+,Q^2)\right\rangle_{q\bar{q}g} &= \sum_{q\bar{q}g,(q\bar{q})_l} |q\bar{q}g\rangle \frac{\langle q\bar{q}g|\,\hat{V}\,|q\bar{q}\rangle_{l\,l}\langle q\bar{q}|\hat{V}\,|\gamma^*\rangle}{\Delta k^-_{02}\Delta k^-_{0l}} + \sum_{q\bar{q}g} |q\bar{q}g\rangle \frac{\langle q\bar{q}g|\,\hat{V}\,|\gamma^*\rangle}{\Delta k^-_{02}} \\ &= \sum_{q\bar{q}g} \frac{b^\dagger d^\dagger a^\dagger\,|0\rangle}{\Delta k^-_{02}} \left[\sum_{\tilde{q}} \frac{\langle 0|\,ab\hat{V}\tilde{b}^\dagger_i\,|0\rangle\,\langle 0|\,d\tilde{b}_i\hat{V}a^\dagger_\gamma\,|0\rangle}{\Delta k^-_{0i}}\right. \\ &\quad \left. + \sum_{\tilde{\bar{q}}} \frac{\langle 0|\,ad\hat{V}\tilde{d}^\dagger_j\,|0\rangle\,\langle 0|\,\tilde{d}_j b\hat{V}a^\dagger_\gamma\,|0\rangle}{\Delta k^-_{0j}} + \langle 0|\,adb\hat{V}a^\dagger_\gamma\,|0\rangle\right].\end{aligned} \tag{3.18}$$

The denominators Δk^-_{kl} are the energy differences between the states k and l. As denoted in Fig. 3.2 the states have the following indices: 0 for initial, 2 for final, i for the intermediary quark and j for the intermediate antiquark state. The total energy of a state l is denoted as $k^-_{l(tot)}$. With this convention the energy denominators become:

$$\begin{aligned}\Delta k^-_{0i} &:= k^-_{0(tot)} - k^-_{i(tot)} = -\frac{Q^2}{2q^+} - k^-_1 - k^-_i \\ \Delta k^-_{0j} &:= k^-_{0(tot)} - k^-_{j(tot)} = -\frac{Q^2}{2q^+} - k^-_0 - k^-_j \\ \Delta k^-_{02} &:= k^-_{0(tot)} - k^-_{2(tot)} = -\frac{Q^2}{2q^+} - k^-_2 - k^-_1 - k^-_0,\end{aligned}$$

where now on the rightmost side the energies are those the constituent particles of the state with the naming convention set in (3.17). Defining the fractional momentum $z_l := k^+_l/q^+$ and using the fact that the longitudinal and transverse momenta are preserved individually, i.e. $q^+ = k^+_1 + k^+_i$ and $0 = \mathbf{q} = \mathbf{k}_1 + \mathbf{k}_i$, we can write

$$\Delta k^-_{0i} = -\frac{1}{2q^+}\frac{1}{z_1(1-z_1)}\left(z_1(1-z_1)Q^2 - \mathbf{k}_1^2\right) \tag{3.19}$$

$$\Delta k^-_{02} = -\frac{1}{2q^+}\left(Q^2 + \frac{\mathbf{k}_0^2}{z_0} + \frac{\mathbf{k}_1^2}{z_1} + \frac{\mathbf{k}_2^2}{z_2}\right), \tag{3.20}$$

and similarly for the intermediate antiquark.

To calculate the $q\bar{q}g$ production amplitude (3.18), we need the vertex rules (3.2)

and (3.3) like in the leading order, the instantaneous QED/QCD production for a transverse photon and gluon emission from either the quark or the antiquark. The rules can be found in [3]. The instantaneous production vertex for the transverse photon is

$$\langle 0|\, adb\hat{V} a_\gamma^\dagger\, |0\rangle = (2\pi)^3 \delta\big(k_0^+ + k_1^+ + k_2^+ - q^+\big)\delta(\mathbf{k}_0 + \mathbf{k}_1 + \mathbf{k}_2 - \mathbf{q}) e e_{f_0} \delta_{f_0,f_1} \delta_{h_0,-h_1}$$
$$\times\, g(T^a)_{A_0 A_1} \sqrt{4k_0^+ k_1^+}\, \delta_{\lambda,\lambda_2} \left[\frac{\delta_{\lambda,-2h_0}}{q^+ - k_1^+} - \frac{\delta_{\lambda,2h_0}}{q^+ - k_0^+} \right], \tag{3.21}$$

and the vertex rule for the gluon emission from the quark is:

$$\langle 0|\, ab\hat{V} b_i^\dagger\, |0\rangle = (2\pi)^3 \delta\big(k_0^+ + k_2^+ - k_i^+\big)\delta(\mathbf{k}_0 + \mathbf{k}_2 - \mathbf{k}_i) \delta_{f_i,f_0} \delta_{h_i,h_0} g(T^a)_{A_0 A_i}$$
$$\times \sqrt{4k_i^+ k_0^+}\, \epsilon_{\lambda_2} \cdot \left[\frac{\mathbf{k}_2}{k_2^+} - \left(\frac{1 + 2h_0\lambda_2}{2} \right) \frac{\mathbf{k}_0}{k_0^+} - \left(\frac{1 - 2h_0\lambda_2}{2} \right) \frac{\mathbf{k}_i}{k_i^+} \right], \tag{3.22}$$

and from the antiquark:

$$\langle 0|\, ad\hat{V} d_j^\dagger\, |0\rangle = (-1)(2\pi)^3 \delta\big(k_1^+ + k_2^+ - k_j^+\big)\delta(\mathbf{k}_1 + \mathbf{k}_2 - \mathbf{k}_j) \delta_{f_j,f_1} \delta_{h_j,h_1} g(T^a)_{A_j A_1}$$
$$\times \sqrt{4k_j^+ k_1^+}\, \epsilon_{\lambda_2} \cdot \left[\frac{\mathbf{k}_2}{k_2^+} - \left(\frac{1 + 2h_0\lambda_2}{2} \right) \frac{\mathbf{k}_1}{k_1^+} - \left(\frac{1 - 2h_0\lambda_2}{2} \right) \frac{\mathbf{k}_j}{k_j^+} \right]. \tag{3.23}$$

In equation (3.18) the formal sum over all possible $q\bar{q}g$ end states entails a summation over the number of partons of each type present in the Fock state and for each parton there is a sum over its quantum numbers and integrations over its phase space, i.e. analogously to the LO case we saw previously with the addition of a gluon in the final state:

$$\sum_{q\bar{q}g\ \ states} \rightsquigarrow \sum_{h_0,A_0,f_0} \sum_{h_1,A_1,f_1} \sum_{\lambda_2,a} \int \frac{dk_0^+}{2\pi 2k_0^+} \int \frac{d^2\mathbf{k}_0}{(2\pi)^2} \int \frac{dk_1^+}{2\pi 2k_1^+} \int \frac{d^2\mathbf{k}_1}{(2\pi)^2} \int \frac{dk_2^+}{2\pi 2k_2^+} \int \frac{d^2\mathbf{k}_2}{(2\pi)^2}. \tag{3.24}$$

Writing out the state sums using (3.24) and inserting the vertex rules (3.2), (3.22), (3.23), (3.21), and energy denominators (3.19),(3.20) into the equation (3.18) we get for the transverse photon wavefunction:

$$
\begin{aligned}
\left|\gamma_T^*(q^+,Q^2)\right\rangle_{q\bar{q}g} = & \sum_{\substack{h_0,h_1,\lambda,\\ A_0,A_i,a,f_0,f_1}} \int\int \frac{dk_0^+}{2\pi 2k_0^+}\frac{d^2\mathbf{k}_0}{(2\pi)^2}\int\int \frac{dk_1^+}{2\pi 2k_1^+}\frac{d^2\mathbf{k}_1}{(2\pi)^2}\int\int \frac{dk_2^+}{2\pi 2k_2^+}\frac{d^2\mathbf{k}_2}{(2\pi)^2} \\
& \times \left\{ \sum_{h_i,A_i,f_i} \int\int \frac{dk_i^+}{2\pi 2k_i^+}\frac{d^2\mathbf{k}_i}{(2\pi)^2} \frac{(2\pi)^3\delta\big(k_0^+ + k_2^+ - k_i^+\big)\delta(\mathbf{k}_0+\mathbf{k}_2-\mathbf{k}_i)\delta_{f_i,f_0}}{-\frac{1}{2q^+}\frac{1}{z_1(1-z_1)}(z_1(1-z_1)Q^2-\mathbf{k}_1^2)} \right. \\
& \times \delta_{h_i,h_0} g(T^a)_{A_0A_i}\sqrt{4k_i^+k_0^+}\epsilon_{\lambda_2}\cdot\left[\frac{\mathbf{k}_2}{k_2^+} - \left(\frac{1+2h_0\lambda_2}{2}\right)\frac{\mathbf{k}_0}{k_0^+} - \left(\frac{1-2h_0\lambda_2}{2}\right)\frac{\mathbf{k}_i}{k_i^+}\right] \\
& \times (2\pi)^3\delta\big(k_i^+ + k_1^+ - q^+\big)\delta(\mathbf{k}_i+\mathbf{k}_1-\mathbf{q})ee_{f_i}\delta_{f_i,f_1}\delta_{A_i,A_1}\delta_{h_i,-h_1}\sqrt{4k_i^+k_1^+} \\
& \times \epsilon_\lambda\cdot\left[\frac{\mathbf{q}}{q^+} - \left(\frac{1+2h_0\lambda}{2}\right)\frac{\mathbf{k}_1}{k_1^+} - \left(\frac{1-2h_0\lambda}{2}\right)\frac{\mathbf{k}_i}{k_i^+}\right] \\
& + (-1)\sum_{h_j,A_j,f_j}\int\int\frac{dk_j^+}{2\pi 2k_j^+}\frac{d^2\mathbf{k}_j}{(2\pi)^2}\frac{(2\pi)^3\delta\big(k_1^+ + k_2^+ - k_j^+\big)\delta(\mathbf{k}_1+\mathbf{k}_2-\mathbf{k}_j)\delta_{f_1,f_j}}{-\frac{1}{2q^+}\frac{1}{z_0(1-z_0)}(z_0(1-z_0)Q^2-\mathbf{k}_0^2)} \\
& \times \delta_{h_j,h_1} g(T^a)_{A_jA_1}\sqrt{4k_0^+k_j^+}\epsilon_{\lambda_2}\cdot\left[\frac{\mathbf{k}_2}{k_2^+} - \left(\frac{1+2h_j\lambda_2}{2}\right)\frac{\mathbf{k}_1}{k_1^+} - \left(\frac{1-2h_j\lambda_2}{2}\right)\frac{\mathbf{k}_j}{k_j^+}\right] \\
& \times (2\pi)^3\delta\big(k_0^+ + k_j^+ - q^+\big)\delta(\mathbf{k}_0+\mathbf{k}_j-\mathbf{q})ee_{f_0}\delta_{f_j,f_0}\delta_{A_0,A_j}\delta_{h_0,-h_j}\sqrt{4k_0^+k_j^+} \\
& \times \epsilon_\lambda\cdot\left[\frac{\mathbf{q}}{q^+} - \left(\frac{1+2h_0\lambda}{2}\right)\frac{\mathbf{k}_j}{k_j^+} - \left(\frac{1-2h_0\lambda}{2}\right)\frac{\mathbf{k}_0}{k_0^+}\right] \\
& + (2\pi)^3\delta\big(k_0^+ + k_1^+ + k_2^+ - q^+\big)\delta(\mathbf{k}_0+\mathbf{k}_1+\mathbf{k}_2-\mathbf{q})ee_{f_0}\delta_{f_0,f_1}\delta_{h_0,-h_1} \\
& \times g(T^a)_{A_0A_1}\sqrt{4k_0^+k_1^+}\delta_{\lambda,\lambda_2}\left[\frac{\delta_{\lambda,-2h_0}}{q^+-k_1^+} - \frac{\delta_{\lambda,2h_0}}{q^+-k_0^+}\right]\Bigg\} \frac{(-2q^+)b^\dagger d^\dagger a^\dagger\left|0\right\rangle}{\left(Q^2+\frac{\mathbf{k}_0^2}{z_0}+\frac{\mathbf{k}_1^2}{z_1}+\frac{\mathbf{k}_2^2}{z_2}\right)}.
\end{aligned}
$$

Carrying out the integrations over the internal momenta, summing over the free quantum numbers and doing a change of integration variable $k_i^+ \to z_i$, we get

$$
\begin{aligned}
&\left|\gamma_T^*(q^+,Q^2)\right\rangle_{q\bar{q}g} \qquad (3.25)\\
&=(-1)\frac{eg}{2(2\pi)^2}\sum_{h_0,\lambda_2}\int\int\int\frac{dz_0}{\sqrt{z_0}}\frac{dz_1}{\sqrt{z_1}}\frac{dz_2}{z_2}\delta(z_0+z_1+z_2-1)\int\int\int\frac{d^2\mathbf{k}_0}{(2\pi)^2}\frac{d^2\mathbf{k}_1}{(2\pi)^2}\frac{d^2\mathbf{k}_2}{(2\pi)^2}\\
&\quad\times\left\{\frac{(\epsilon_\lambda\cdot\mathbf{k}_1)[1-2z_1+2h_0\lambda]}{z_1(1-z_1)Q^2+\mathbf{k}_1^2}\frac{1-z_1}{1-z_1-z_2}\left[1-\frac{z_2}{1-z_1}\left(\frac{1-2h_0\lambda_2}{2}\right)\right]\epsilon_{\lambda_2}^*\cdot\left[\frac{\mathbf{k}_2}{z_2}+\frac{\mathbf{k}_1}{1-z_1}\right]\right.\\
&\quad-\frac{(\epsilon_\lambda\cdot\mathbf{k}_0)[1-2z_+-2h_0\lambda]}{z_0(1-z_0)Q^2+\mathbf{k}_0^2}\frac{1-z_0}{1-z_0-z_2}\left[1-\frac{z_2}{1-z_0}\left(\frac{1+2h_0\lambda_2}{2}\right)\right]\epsilon_{\lambda_2}^*\cdot\left[\frac{\mathbf{k}_2}{z_2}+\frac{\mathbf{k}_0}{1-z_0}\right]\\
&\quad\left.+\,\delta_{\lambda,\lambda_2}\left[\frac{\delta_{\lambda,-2h_0}}{1-z_1}-\frac{\delta_{\lambda,2h_0}}{1-z_0}\right]\right\}\times\frac{(2\pi)^2\delta(\mathbf{k}_0+\mathbf{k}_1+\mathbf{k}_2)}{Q^2+\frac{\mathbf{k}_0^2}{z_0}+\frac{\mathbf{k}_1^2}{z_1}+\frac{\mathbf{k}_2^2}{z_2}}\\
&\quad\times\sum_f e_f\sum_{a,A_0,A_1}(T^a)_{A_0A_1}b^\dagger d^\dagger a^\dagger\left|0\right\rangle,
\end{aligned}
$$

where now due to the conservations imposed by the delta structure, the quarks have opposing helicities:

$$
b^\dagger d^\dagger a^\dagger\left|0\right\rangle=b^\dagger\big(k_0^+,\mathbf{k}_0,h_0,A_0,f\big)d^\dagger\big(k_1^+,\mathbf{k}_1,-h_0,A_1,f\big)a^\dagger\big(k_2^+,\mathbf{k}_2,\lambda_2,a\big)\left|0\right\rangle.
$$

Via a similar calculation we get for the longitudinally polarized photon, using its specific vertex rule (3.3):

$$
\begin{aligned}
&\left|\gamma_L^*(q^+,Q^2)\right\rangle_{q\bar{q}g}\\
&\quad=\frac{egQ}{(2\pi)^2}\sum_{h_0,\lambda_2}\int\int\int\frac{dz_0}{\sqrt{z_0}}\frac{dz_1}{\sqrt{z_1}}\frac{dz_2}{z_2}\delta(z_0+z_1+z_2-1)\int\int\int\frac{d^2\mathbf{k}_0}{(2\pi)^2}\frac{d^2\mathbf{k}_1}{(2\pi)^2}\frac{d^2\mathbf{k}_2}{(2\pi)^2}\\
&\qquad\times\left\{\frac{z_1(1-z_1)^2}{1-z_1-z_2}\left[1-\frac{z_2}{1-z_1}\left(\frac{1-2h_0\lambda_2}{2}\right)\right]\frac{\epsilon_{\lambda_2}^*\cdot\left[\frac{\mathbf{k}_2}{z_2}+\frac{\mathbf{k}_1}{1-z_1}\right]}{z_1(1-z_1)Q^2+\mathbf{k}_1^2}\right.\\
&\qquad\left.-\,\frac{z_0(1-z_0)^2}{1-z_0-z_2}\left[1-\frac{z_2}{1-z_0}\left(\frac{1+2h_0\lambda_2}{2}\right)\right]\frac{\epsilon_{\lambda_2}^*\cdot\left[\frac{\mathbf{k}_2}{z_2}+\frac{\mathbf{k}_0}{1-z_0}\right]}{z_0(1-z_0)Q^2+\mathbf{k}_0^2}\right\}\\
&\qquad\times\frac{(2\pi)^2\delta(\mathbf{k}_0+\mathbf{k}_1+\mathbf{k}_2)}{Q^2+\frac{\mathbf{k}_0^2}{z_0}+\frac{\mathbf{k}_1^2}{z_1}+\frac{\mathbf{k}_2^2}{z_2}}\times\sum_f e_f\sum_{a,A_0,A_1}(T^a)_{A_0A_1}b^\dagger d^\dagger a^\dagger\left|0\right\rangle,
\end{aligned}
\qquad (3.26)
$$

where there are only two terms due to the absence of the instantaneous splitting. From both equations (3.25) and (3.26) one can see that the quark to gluon and

antiquark to gluon emissions have a relative sign difference and thus they cancel each other out at low gluon transverse momentum limit, as they should.

Next we'll Fourier transform the results (3.25) and (3.26) into mixed space of the fractional momenta and particle positions – $(z_0, z_1, z_2, \mathbf{x}_0, \mathbf{x}_1, \mathbf{x}_2)$. To do this, we need the operator Fourier transformation relation (2.11) and a couple of integration formulae. Define $x_{ij} := x_i - x_j$ and

$$\int dZ := \int\int\int \frac{dz_0}{\sqrt{z_0}}\frac{dz_1}{\sqrt{z_1}}\frac{dz_2}{z_2}\delta(z_0+z_1+z_2-1).$$

With these definitions the necessary integration formulae are [3]:

$$\begin{aligned}
&\int\int \frac{d^2\mathbf{k}_1}{2\pi}\frac{d^2\mathbf{k}_2}{2\pi}\frac{e^{i(\mathbf{k}_1\cdot\mathbf{x}_{10}+\mathbf{k}_2\cdot\mathbf{x}_{20})}k_1^\mu\left(\frac{k_2^\nu}{z_2}+\frac{k_1^\nu}{1-z_1}\right)}{(z_1(1-z_1)Q^2+\mathbf{k}_1^2)\left(Q^2+\frac{(\mathbf{k}_1+\mathbf{k}_2)^2}{1-z_1-z_2}+\frac{\mathbf{k}_1^2}{z_1}+\frac{\mathbf{k}_2^2}{z_2}\right)} \\
&= -z_1(1-z_1-z_2)\left(x_{10}^\mu-\frac{z_2}{1-z_1}x_{20}^\mu\right)\frac{x_{20}^\nu}{|x_{20}|^2}\frac{QXK_1(QX)}{X^2} \qquad (3.27)\\
&\int\int \frac{d^2\mathbf{k}_1}{2\pi}\frac{d^2\mathbf{k}_2}{2\pi}\frac{e^{i(\mathbf{k}_1\cdot\mathbf{x}_{10}+\mathbf{k}_2\cdot\mathbf{x}_{20})}}{\left(Q^2+\frac{(\mathbf{k}_1+\mathbf{k}_2)^2}{1-z_1-z_2}+\frac{\mathbf{k}_1^2}{z_1}+\frac{\mathbf{k}_2^2}{z_2}\right)} \\
&= z_2z_1(1-z_1-z_2)\frac{QXK_1(QX)}{X^2} \qquad (3.28)\\
&\int\int \frac{d^2\mathbf{k}_1}{2\pi}\frac{d^2\mathbf{k}_2}{2\pi}\frac{e^{i(\mathbf{k}_1\cdot\mathbf{x}_{10}+\mathbf{k}_2\cdot\mathbf{x}_{20})}\left(\frac{k_2^\nu}{z_2}+\frac{k_1^\nu}{1-z_1}\right)}{(z_1(1-z_1)Q^2+\mathbf{k}_1^2)\left(Q^2+\frac{(\mathbf{k}_1+\mathbf{k}_2)^2}{1-z_1-z_2}+\frac{\mathbf{k}_1^2}{z_1}+\frac{\mathbf{k}_2^2}{z_2}\right)} \\
&= i\frac{1-z_1-z_2}{1-z_1}\frac{x_{20}^\nu}{|x_{20}|^2}K_0(QX). \qquad (3.29)
\end{aligned}$$

Here K_0 and K_1 are the 0th and 1st modified Bessel functions of the second kind and X is shorthand for

$$\begin{aligned}
X &= z_1(1-z-1)\left(\mathbf{x}_{10}-\frac{z_2}{1-z_1}\mathbf{x}_{20}\right)^2+\frac{z_2(1-z_1-z_2)}{1-z_1}|x_{20}|^2 \\
&= z_0(1-z-0)\left(\mathbf{x}_{01}-\frac{z_2}{1-z_0}\mathbf{x}_{21}\right)^2+\frac{z_2(1-z_0-z_2)}{1-z_0}|x_{21}|^2 \\
&= z_0z_1|x_{10}|^2+z_0z_2|x_{20}|^2+z_1z_2|x_{21}|^2,
\end{aligned}$$

where the equalities hold when the momentum fraction conservation $z_0+z_1+z_2=1$ holds. These integration relations, in addition to the relations (3.7) and (3.8) needed in the LO calculation, can be derived by using the Schwinger representation for the denominators.

Substituting the Fourier relation (2.11) into the phase space amplitude (3.25) we get with the above formulae for the Fourier transform

$$
\begin{aligned}
&\mathcal{F}\left|\gamma_T^*(q^+,Q^2)\right\rangle_{q\bar{q}g} \qquad (3.30)\\
&= (-1)\frac{eg}{2(2\pi)^2}\sum_{h_0,\lambda_2}\int dZ\prod_{i=0}^{2}\left(\int\frac{d^2\mathbf{k}_i}{(2\pi)^2}\right)\left(\int\frac{d^2\mathbf{x}_i}{2\pi}\right)e^{i(\mathbf{k}_0\cdot\mathbf{x}_0+\mathbf{k}_1\cdot\mathbf{x}_1+\mathbf{k}_2\cdot\mathbf{x}_2)}\\
&\quad\times\left\{\frac{(\epsilon_\lambda\cdot\mathbf{k}_1)[1-2z_1+2h_0\lambda]}{z_1(1-z_1)Q^2+\mathbf{k}_1^2}\frac{1-z_1}{1-z_1-z_2}\left[1-\frac{z_2}{1-z_1}\left(\frac{1-2h_0\lambda_2}{2}\right)\right]\epsilon_{\lambda_2}^*\cdot\left[\frac{\mathbf{k}_2}{z_2}+\frac{\mathbf{k}_1}{1-z_1}\right]\right.\\
&\quad-\frac{(\epsilon_\lambda\cdot\mathbf{k}_0)[1-2z_+-2h_0\lambda]}{z_0(1-z_0)Q^2+\mathbf{k}_0^2}\frac{1-z_0}{1-z_0-z_2}\left[1-\frac{z_2}{1-z_0}\left(\frac{1+2h_0\lambda_2}{2}\right)\right]\epsilon_{\lambda_2}^*\cdot\left[\frac{\mathbf{k}_2}{z_2}+\frac{\mathbf{k}_0}{1-z_0}\right]\\
&\quad\left.+\,\delta_{\lambda,\lambda_2}\left[\frac{\delta_{\lambda,-2h_0}}{1-z_1}-\frac{\delta_{\lambda,2h_0}}{1-z_0}\right]\right\}\times\frac{(2\pi)^2\delta(\mathbf{k}_0+\mathbf{k}_1+\mathbf{k}_2)}{Q^2+\frac{\mathbf{k}_0^2}{z_0}+\frac{\mathbf{k}_1^2}{z_1}+\frac{\mathbf{k}_2^2}{z_2}}\\
&\quad\times\sum_f e_f\sum_{a,A_0,A_1}(T^a)_{A_0A_1}b^\dagger d^\dagger a^\dagger\left|0\right\rangle
\end{aligned}
$$

where integrating first over $d^2\mathbf{k}_0$ in the first and third terms and over $d^2\mathbf{k}_1$ in the second term, renders the equation into a form where we can take advantage of the Fourier integrals given, ultimately yielding

$$
\begin{aligned}
&\mathcal{F}\left|\gamma_{T,L}^*(q^+,Q^2)\right\rangle_{q\bar{q}g}\\
&\quad=\frac{eg}{4\pi}\sum_{h_0,\lambda_2}\int\int\int\frac{dz_0}{\sqrt{z_0}}\frac{dz_1}{\sqrt{z_1}}\frac{dz_2}{z_2}\delta(z_0+z_1+z_2-1)\int\int\int\frac{d^2\mathbf{x}_0}{(2\pi)^2}\frac{d^2\mathbf{x}_1}{(2\pi)^2}\frac{d^2\mathbf{x}_2}{(2\pi)^2}\\
&\qquad\times\Phi_{T,L}(z_0,z_1,z_2,\mathbf{x}_0,\mathbf{x}_1,\mathbf{x}_2,h_0,\lambda_2,\lambda)\\
&\qquad\times\sum_f e_f\sum_{a,A_0,A_1}(T^a)_{A_0A_1}b^\dagger(x_0)d^\dagger(x_1)a^\dagger(x_2)\left|0\right\rangle,
\end{aligned}
\qquad (3.31)
$$

where we have for the transverse polarization

$$\Phi_T(z_0,z_1,z_2,\mathbf{x}_0,\mathbf{x}_1,\mathbf{x}_2,h_0,\lambda_2,\lambda) = \frac{QXK_1(QX)}{X^2}\times \tag{3.32}$$
$$\Bigg\{\ z_1(1-z_1)[1-2z_1+2h_0\lambda]\left[1-\frac{z_2}{1-z_1}\left(\frac{1-2h_0\lambda_2}{2}\right)\right]\epsilon_\lambda\cdot\left[\mathbf{x}_{10}\frac{z_2}{1-z_1}\mathbf{x}_{20}\right]\frac{\epsilon^*_{\lambda_2}\cdot\mathbf{x}_{20}}{|x_{20}|^2}$$
$$-\ z_0(1-z_0)[1-2z_0-2h_0\lambda]\left[1-\frac{z_2}{1-z_0}\left(\frac{1+2h_0\lambda_2}{2}\right)\right]\epsilon_\lambda\cdot\left[\mathbf{x}_{01}\frac{z_2}{1-z_0}\mathbf{x}_{21}\right]\frac{\epsilon^*_{\lambda_2}\cdot\mathbf{x}_{21}}{|x_{21}|^2}$$
$$-\ z_0z_1z_2\delta_{\lambda,\lambda_2}\left[\frac{\delta_{\lambda,-2h_0}}{1-z_1}-\frac{\delta_{\lambda,2h_0}}{1-z_0}\right]\Bigg\}.$$

With a similar calculation we get for the longitudinal polarization case the same structure (3.31) as for the transverse case, which was already denoted there, with

$$\Phi_L(z_0,z_1,z_2,\mathbf{x}_0,\mathbf{x}_1,\mathbf{x}_2,h_0,\lambda_2,\lambda) = 2iQK_0(QX)\times \tag{3.33}$$
$$\Bigg\{\ z_1(1-z_1)\left[1-\frac{z_2}{1-z_1}\left(\frac{1-2h_0\lambda_2}{2}\right)\right]\frac{\epsilon^*_{\lambda_2}\cdot\mathbf{x}_{20}}{|x_{20}|^2}$$
$$-z_0(1-z_0)\left[1-\frac{z_2}{1-z_0}\left(\frac{1+2h_0\lambda_2}{2}\right)\right]\frac{\epsilon^*_{\lambda_2}\cdot\mathbf{x}_{21}}{|x_{21}|^2}\Bigg\}.$$

Now with the photon splitting amplitudes in the mixed-space, i.e. the result (3.31) with the polarization dependent pieces (3.32) and (3.33), we still need to handle the NLO $q\bar{q}$ contribution before we can move on to compute the cross section.

3.3 Virtual contribution problems

We now have calculated one of the two next-to-leading order contributions to the virtual photon splitting wavefunction, namely the loopless contribution. The remaining pieces are the one-loop interactions with the target. In these processes the virtual photon splits into a quark-antiquark-gluon triplet either instantly or in two steps and the internal gluon is reabsorbed before the interaction instant by either of the quarks, forming a loop. There are nine such diagrams which are shown in Fig. 3.3. Every diagram is relevant for a transversely polarized virtual photon whereas only the first five, Figs. 3.3a – 3.3e, are to be considered for a longitudinally polarized photon due to the instantaneous vertex in the remaining diagrams that is forbidden for a longitudinal virtual photon.

An explicit calculation of the one-loop diagrams is a cumbersome task, so the article [3], that much of this study follows, tried to work their way past it with an argument based on unitarity and normalization. The idea was to deduce a relation between the LO and the two NLO contributions $q\bar{q}$ and $q\bar{q}g$ from a truncated Fock state expansion of the full photon wavefunction by imposing that the normalizations of the LO and NLO wavefunctions are the same so that probability would be conserved. However, it has since been realized that the workaround is flawed [10]. The issue is a bit subtle so let us look at this in better detail to give an idea where the problem lies. We start from the Fock expansion of the full photon wavefunction:

$$\begin{aligned} |\gamma(\mathbf{q},\lambda)\rangle &= \sqrt{Z_\gamma}\left[a_\gamma^\dagger|0\rangle + \sum_{\mathcal{F}\neq\gamma}\Psi_{\gamma\to\mathcal{F}}|\mathcal{F}\rangle\right] \\ &= \sqrt{Z_\gamma}\left[a_\gamma^\dagger|0\rangle + \sum_{\mathcal{F}=l\bar{l}}\Psi_{\gamma\to l_0\bar{l}_1}b_{l,0}^\dagger d_{l,1}^\dagger|0\rangle\right. \\ &\quad \left. + \sum_{\mathcal{F}=q\bar{q}}\Psi_{\gamma\to q_0\bar{q}_1}b_0^\dagger d_1^\dagger|0\rangle + \sum_{\mathcal{F}=q\bar{q}g}\Psi_{\gamma\to q_0\bar{q}_1 g_2}b_0^\dagger d_1^\dagger a_2^\dagger|0\rangle + \ldots,\right] \end{aligned} \tag{3.34}$$

where the expansion was truncated after NLO relevant particle compositions and the arguments of the particle operators were left implicit, in the same vein as was done with the loopless diagram calculation. The full state is normalized as

$$\langle\gamma(\mathbf{q}',\lambda')|\gamma(\mathbf{q},\lambda)\rangle = 2q^+(2\pi)^3\delta^{(3)}(\underline{q}'-\underline{q})\delta_{\lambda',\lambda}, \tag{3.35}$$

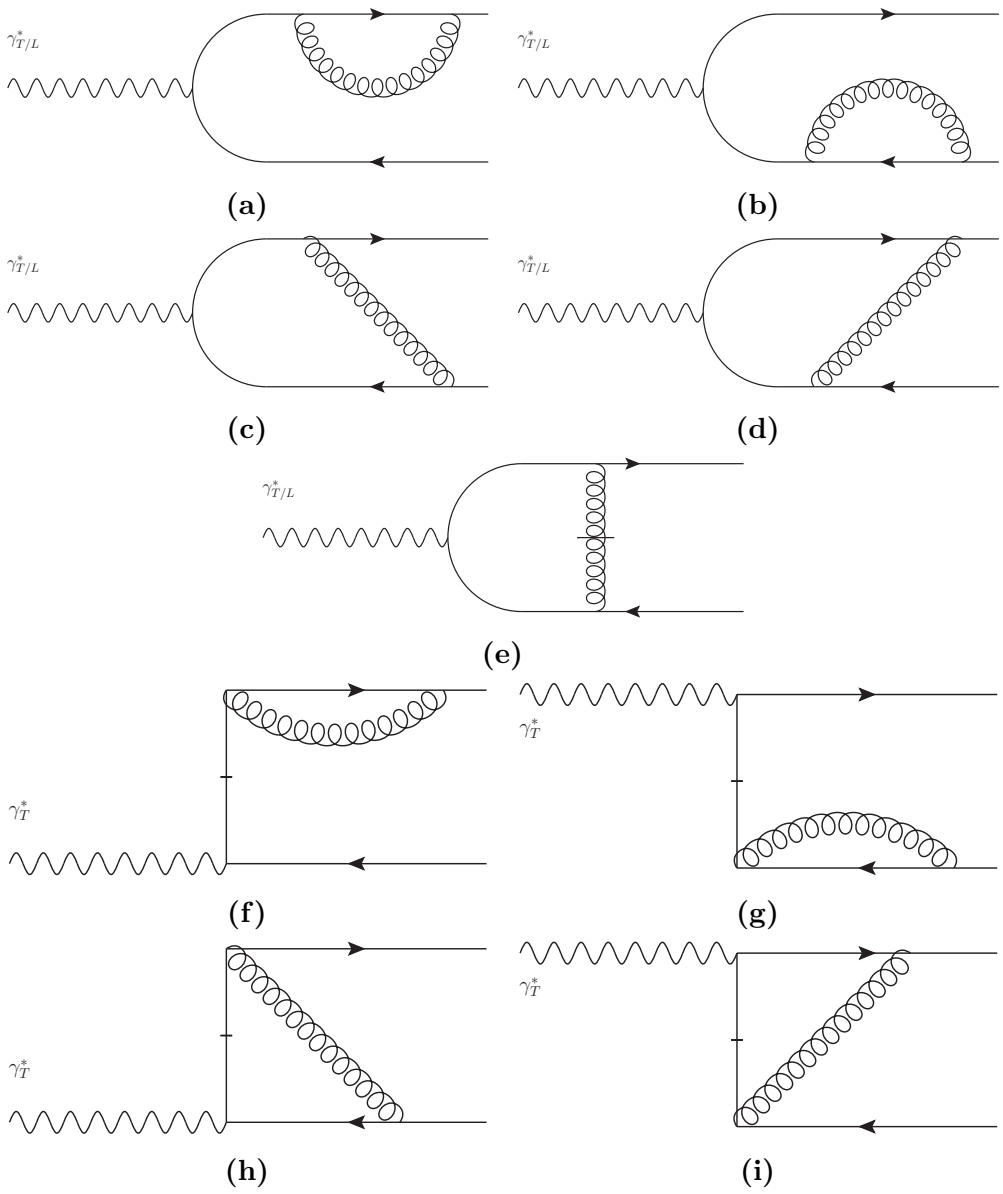

Figure 3.3: The nine possible virtual process diagrams to be considered in the next-to-leading order calculation. In figures (a)–(e) the virtual photon first splits in a QED process into the quark-antiquark pair after which either of the quarks emits a gluon that is then absorbed elsewhere. In figures (f)–(i) the photon splits at once into a quark-antiquark-gluon state in an instantaneous QED/QCD process after which the gluon is absorbed. In the latter four diagrams only a transverse photon is allowed to take a part in the instantaneous vertex. The diagrams are ordered horizontally in light cone time x^+, the initial state $x^+ = -\infty$ being on the left edge of each diagram and the interaction instant $x^+ = 0$ being on the right.

where the definition

$$\underline{q} \coloneqq \big(q^+, q_T\big)$$

has been made. Using this and the orthogonality of the Fock space basis, we can calculate the square of the modulus of either side in (3.34) to get, after moving the pure photon state to the left side, a unitarity relation:

$$\begin{aligned} 2q^+(2\pi)^3\delta^{(3)}(\underline{q}'-\underline{q})\delta_{\lambda',\lambda}\frac{1-Z_\gamma}{Z_\gamma} = &\sum_{\mathcal{F}=l\bar{l}}\big(\Psi_{\gamma'\to l_0\bar{l}_1}\big)^\dagger\Psi_{\gamma\to l_0\bar{l}_1} + \sum_{\mathcal{F}=q\bar{q}}\big(\Psi_{\gamma'\to q_0\bar{q}_1}\big)^\dagger\Psi_{\gamma\to q_0\bar{q}_1} \\ &+ \sum_{\mathcal{F}=q\bar{q}g}\big(\Psi_{\gamma'\to q_0\bar{q}_1 g_2}\big)^\dagger\Psi_{\gamma\to q_0\bar{q}_1 g_2} \\ &+ \mathcal{O}\big(\alpha_{em}\alpha_s^2\big) + \mathcal{O}\big(\alpha_{em}^2\big). \end{aligned} \tag{3.36}$$

In this expansion, on the right hand side the first term cannot have a contribution of the order $\alpha_{em}\alpha_s$ so when we specifically compare the NLO terms that are of the order $\alpha_{em}\alpha_s$ we can ignore the lepton-lepton contribution in its entirety, and similarly the remaining terms that are of higher order. We get

$$\begin{aligned} 2q^+(2\pi)^3\delta^{(3)}(\underline{q}'-\underline{q})\delta_{\lambda',\lambda}\left(\frac{1-Z_\gamma}{Z_\gamma}\right)_{\alpha_{em}\alpha_s} = &\left(\sum_{\mathcal{F}=q\bar{q}}\big(\Psi_{\gamma'\to q_0\bar{q}_1}\big)^\dagger\Psi_{\gamma\to q_0\bar{q}_1}\right)_{\alpha_{em}\alpha_s} \\ &+ \left(\sum_{\mathcal{F}=q\bar{q}g}\big(\Psi_{\gamma'\to q_0\bar{q}_1 g_2}\big)^\dagger\Psi_{\gamma\to q_0\bar{q}_1 g_2}\right)_{\alpha_{em}\alpha_s}. \end{aligned} \tag{3.37}$$

Now the NLO $q\bar{q}$ contribution is inferred from the relation

$${}_{LO}\big\langle\gamma^*_{T,L}\big|\gamma^*_{T,L}\big\rangle_{LO} = {}_{NLO}\big\langle\gamma^*_{T,L}\big|\gamma^*_{T,L}\big\rangle_{NLO} = {}_{q\bar{q}}\big\langle\gamma^*_{T,L}\big|\gamma^*_{T,L}\big\rangle_{q\bar{q}} + {}_{q\bar{q}g}\big\langle\gamma^*_{T,L}\big|\gamma^*_{T,L}\big\rangle_{q\bar{q}g}$$

using the known LO and $q\bar{q}g$ results. However, this implicitly assumes that the left hand side in Fourier transformed mixed-space counterpart of (3.37) vanishes. This is the breaking point for the approach, since the normalization factor on the l.h.s. receives a finite correction in the order $\alpha_{em}\alpha_s$ and hence does not vanish at that specific order. Thus the unitarity relation cannot be used to deduce the $q\bar{q}$ contribution from the two directly calculated results.

The one-loop corrections have both UV and soft divergences. Due to the UV divergence they have to be renormalized using something else than a cut-off, which has been done with dimensional regularization [10]. This UV divergence must cancel with a UV divergence in the $q\bar{q}g$ contribution when the contributions are combined. The soft divergence on the other hand is similar to the one in the loopless NLO contribution, so one might also try a cut-off regularization similarly as will be done in Section 3.5 here.

These explicit loop calculations are out of the scope for this work and so we will be mindful of the details mentioned above and use the result from [3] in the numerical examinations done in this work. In Section 3.4 we will write the result in a way that when the loop calculation results are done and verified they are easy to implement as a modular addition to the work done here. The verification and implementation of the full one-loop result is one of the two significant undertakings that is left to be done beyond this work.

3.4 Photon cross sections

In this section we will calculate the polarized cross sections for a virtual photon scattering from a gluon field using the LO and NLO results of Sections 3.1 and 3.2. The optical theorem (2.24) states that the polarized cross section is

$$\sigma^{\gamma}_{T,L}[\mathcal{A}] = \frac{1}{2\pi q^+ \delta(q'^+ - q^+)} \operatorname{Re}\Big({}_{NLO}\big\langle \gamma^*_{T,L} \big|\, 1 - \hat{S}_E \,\big|\gamma^*_{T,L}\big\rangle_{NLO} \Big). \tag{3.38}$$

To simplify this we will require that both the LO and NLO states have the same normalization:

$${}_{LO}\big\langle \gamma^*_{T,L} \big| \gamma^*_{T,L} \big\rangle_{LO} = {}_{NLO}\big\langle \gamma^*_{T,L} \big| \gamma^*_{T,L} \big\rangle_{NLO} = {}_{q\bar{q}}\big\langle \gamma^*_{T,L} \big| \gamma^*_{T,L} \big\rangle_{q\bar{q}} + {}_{q\bar{q}g}\big\langle \gamma^*_{T,L} \big| \gamma^*_{T,L} \big\rangle_{q\bar{q}g} \tag{3.39}$$

and the facts that in the eikonal approximation the scattering matrix element for the colorless projectile is real and it does not affect the parton composition of the state, i.e. that taking the real part is redundant and that the particle composition of the dipole is left untouched in the scattering. With these we can then break the cross section into separate parts:

$$\begin{aligned}
&\sigma^{\gamma}_{T,L}[\mathcal{A}] \\
&= \frac{1}{2\pi\delta\Big(\frac{q'^+}{q^+} - 1\Big)} \Big[{}_{NLO}\big\langle \gamma^*_{T,L} \big| \gamma^*_{T,L} \big\rangle_{NLO} - {}_{NLO}\big\langle \gamma^*_{T,L} \big|\, \hat{S}_E \,\big| \gamma^*_{T,L} \big\rangle_{NLO} \Big] \\
&= \frac{1}{2\pi\delta\Big(\frac{q'^+}{q^+} - 1\Big)} \Big[{}_{LO}\big\langle \gamma^*_{T,L} \big| \gamma^*_{T,L} \big\rangle_{LO} - {}_{q\bar{q}}\big\langle \gamma^*_{T,L} \big|\, \hat{S}_E \,\big| \gamma^*_{T,L} \big\rangle_{q\bar{q}} - {}_{q\bar{q}g}\big\langle \gamma^*_{T,L} \big|\, \hat{S}_E \,\big| \gamma^*_{T,L} \big\rangle_{q\bar{q}g} \Big],
\end{aligned} \tag{3.40}$$

where the first term is the leading order dominating contribution, the second is the NLO $q\bar{q}$ contribution from the virtual graphs with closed gluon loops and the third is the other NLO contribution from the quark antiquark gluon graphs. As discussed in Section 3.3, we will calculate the NLO cross section using the directly calculated $q\bar{q}g$ contribution of the real graphs and the place holder virtual contribution from [3].

Let us calculate first the leading order dominating contribution of the cross section. For this we need the Fourier transformed LO splitting amplitude (3.9) calculated in Section 3.1. Writing out the scalar overlap of the LO initial and final

states we get

$$
\begin{aligned}
&{}_{LO}\Big\langle \gamma^*_{(T),L}(q^{'+})\Big|\gamma^*_{(T),L}(q^+)\Big\rangle_{LO} = \frac{e^2}{4}\int_0^1\int_0^1 \frac{dz_0'}{\sqrt{z_0'}}\frac{dz_1'}{\sqrt{z_1'}}\delta(z_0'+z_1'-1) \qquad (3.41)\\
&\times \int_0^1\int_0^1 \frac{dz_0}{\sqrt{z_0}}\frac{dz_1}{\sqrt{z_1}}\delta(z_0+z_1-1)\int\frac{d^2\mathbf{x}_0'}{(2\pi)^2}\int\frac{d^2\mathbf{x}_1'}{(2\pi)^2}\int\frac{d^2\mathbf{x}_0}{(2\pi)^2}\int\frac{d^2\mathbf{x}_1}{(2\pi)^2}\\
&\times \left[\sum_{h_0'}\Phi^{LO}_{(T),L}(\mathbf{x}_0',..)^\dagger\right]\left[\sum_{h_0}\Phi^{LO}_{(T),L}(\mathbf{x}_0,..)\right]\times\sum_{f,f'}e_f e_{f'}\\
&\times \sum_{A_0,A_0'}\langle 0|\, d(\mathbf{x}_1',-h_0'..)b(\mathbf{x}_0',h_0',..)b^\dagger(\mathbf{x}_0,h_0,..)d^\dagger(\mathbf{x}_1,-h_0,..)\,|0\rangle\,.
\end{aligned}
$$

To evaluate the matrix element, we need the fermion anticommutation relations (2.8); after two anticommutations and two annihilated vacuums we get

$$
\begin{aligned}
\langle 0|\, d(\mathbf{x}_1',..)b(\mathbf{x}_0',..)b^\dagger(\mathbf{x}_0,..)d^\dagger(\mathbf{x}_1,..)\,|0\rangle &= (2\pi)^6 2^2 k_0^+ k_1^+ \delta\Big(k_0^+ - k_0^{'+}\Big)\delta\Big(k_1^+ - k_1^{'+}\Big)\\
&\times \delta^{(2)}(\mathbf{x}_0-\mathbf{x}_0')\delta^{(2)}(\mathbf{x}_1-\mathbf{x}_1')\\
&\times \delta^{h_0,h_0'}\delta^{-h_0,-h_0'}\delta^{A_0,A_0'}\delta^{A_0,A_0'}\delta^{f_0,f_0'}\delta^{f_0,f_0'}.
\end{aligned}
\qquad (3.42)
$$

We see that the sums over quark flavors and colors separate and that the integrals over the initial transverse positions are trivial. For the less obvious color sum factor we get

$$
\begin{aligned}
\sum_{A_0,A_0'}\delta^{A_0,A_0'}\delta^{A_0,A_0'} &= \sum_{A_0'}\delta^{A_0',A_0'}\\
&= N_c.
\end{aligned}
\qquad (3.43)
$$

The momentum deltas need to be written in terms of the fractional momenta:

$$
\delta\Big(k_i^+ - k_i^{'+}\Big) = \frac{1}{q^+}\delta\left(z_i^+ - z_i^{'+}\frac{q^{'+}}{q^+}\right). \qquad (3.44)
$$

Plugging these into (3.41) and simplifying after integrating over $z_0, z_1, \mathbf{x}_0, \mathbf{x}_1$ we get

$$
\begin{aligned}
&{}_{LO}\Big\langle \gamma^*_{(T),L}(q^{'+})\Big|\gamma^*_{(T),L}(q^+)\Big\rangle_{LO} = \frac{e^2}{4}\frac{N_c 2^2}{(2\pi)^2}\sum_f e_f^2\int_0^1\int_0^1 dz_0' dz_1'\frac{q^{'+}}{q^+}\delta(z_0'+z_1'-1)\\
&\times\delta\left(\frac{q^{'+}}{q^+}(z_0'+z_1')-1\right)\int d^2\mathbf{x}_0'\int d^2\mathbf{x}_1'\sum_{h_0'}\left[\Phi^{LO}_{(T),L}(\mathbf{x}_0',z_0',..)^\dagger\Phi^{LO}_{(T),L}\left(\mathbf{x}_0',\frac{q^{'+}}{q^+}z_0',..\right)\right].
\end{aligned}
\qquad (3.45)
$$

Integrating over z_0' to get rid of one of the fractional momentum deltas we get

$$
\begin{aligned}
{}_{LO}\Big\langle \gamma^*_{(T),L}(q^{'+})\Big|\gamma^*_{(T),L}(q^+)\Big\rangle_{LO} &= \frac{e^2}{4}\frac{N_c 2^2}{(2\pi)^2}\sum_f e_f^2 \int_0^1 dz_1' \frac{q^{'+}}{q^+}\delta\left(\frac{q^{'+}}{q^+}-1\right) \\
\times \int d^2\mathbf{x}_0' \int d^2\mathbf{x}_1' \sum_{h_0'} &\left[\Phi^{LO}_{(T),L}(\mathbf{x}_0', z_0', ..)^\dagger \Phi^{LO}_{(T),L}\left(\mathbf{x}_0', \frac{q^{'+}}{q^+}z_0', ..\right)\right].
\end{aligned}
\tag{3.46}
$$

Using the photon momentum delta to set the ratio $q^{'+}/q^+$ to unity elsewhere we get the final result:

$$
\begin{aligned}
{}_{LO}\Big\langle \gamma^*_{(T),L}(q^{'+})\Big|\gamma^*_{(T),L}(q^+)\Big\rangle_{LO} &= 2\pi\frac{2\alpha_{em}N_c}{(2\pi)^2}\delta\left(\frac{q^{'+}}{q^+}-1\right)\sum_f e_f^2 \\
\times \int_0^1 dz_1 \int d^2\mathbf{x}_0 \int d^2\mathbf{x}_1 \sum_{h_0} &\left|\Phi^{LO}_{(T),L}(\mathbf{x}_0, \mathbf{x}_1, 1-z_1, z_1, h_0, (\lambda))\right|^2,
\end{aligned}
\tag{3.47}
$$

where the superfluous primes of the integration variables were dropped and the unsimplified prefactor was left so that the cancellations when evaluating the cross section itself will be obvious.

Let us compute next the real graph contribution. Taking the mixed space result (3.31) we get using the introduced shorthand notation

$$
\begin{aligned}
{}_{q\bar{q}g}\big\langle \gamma^*_{(T),L}\big|\, \hat{S}_E \,\big|\gamma^*_{(T),L}\big\rangle_{q\bar{q}g} = \left(\frac{eg}{4\pi}\right)^2 &\sum_{h_0,\lambda_2,(\lambda)} \sum_{h_0',\lambda_2',(\lambda')} \int\int dZ dZ' \prod_{i=0}^{2}\left(\int \frac{d^2\mathbf{x}_i}{2\pi}\int \frac{d^2\mathbf{x}_i'}{2\pi}\right) \\
&\times \Phi^*_{(T),L}(z_0', \dots)\Phi_{(T),L}(z_0, \dots) \\
&\times \sum_f e_f \sum_{f'} e_{f'} \left(\sum_{a',A_0',A_1'} \left(T^{a'}\right)_{A_0'A_1'}\right)^\dagger \sum_{a,A_0,A_1} (T^a)_{A_0A_1} \\
&\times \langle 0|\, a(x_2')d(x_1')b(x_0')\, \hat{S}_E\, b^\dagger(x_0)d^\dagger(x_1)a^\dagger(x_2)\,|0\rangle\,.
\end{aligned}
\tag{3.48}
$$

To evaluate this, we need the creation and annihilation operator anticommutation relations (2.8) and (2.9) for the partons in the dipole and the fact that the eikonal scattering operator $\hat{S}_E$ acts by rotating the colors of the Fock state's partons by a

Wilson line defined along the parton's trajectory through the target [3, 5]:

$$\begin{aligned}
&\hat{S}_E\; b^\dagger(\mathbf{x}_0, A_0) d^\dagger(\mathbf{x}_1, A_1) a^\dagger(\mathbf{x}_2, a)\,|0\rangle \\
&\quad = \sum_{B_0, B_1, b} [U(\mathbf{x}_0)]_{B_0 A_0} \left[U^\dagger(\mathbf{x}_1)\right]_{A_1 B_1} [V(\mathbf{x}_2)]_{ba} b^\dagger(\mathbf{x}_0, B_0) d^\dagger(\mathbf{x}_1, B_1) a^\dagger(\mathbf{x}_2, b)\,|0\rangle \\
&\quad =: \mathcal{W}\left(\mathbf{x}_0, B_0, \dots\right) b^\dagger(\mathbf{x}_0, B_0) d^\dagger(\mathbf{x}_1, B_1) a^\dagger(\mathbf{x}_2, b)\,|0\rangle\,,
\end{aligned} \tag{3.49}$$

where the fundamental and adjoint Wilson lines are respectively defined as path ordered exponentials for a classical shockwave $\mathcal{A}$ [5]:

$$\begin{aligned}
U(\mathbf{x}) &:= U[\mathcal{A}](\mathbf{x}) := \mathcal{P} \exp\left[ig \int dx^+ T^a \mathcal{A}_a^-(x^+, \mathbf{x}, 0)\right] \\
V(\mathbf{x}) &:= V[\mathcal{A}](\mathbf{x}) := \mathcal{P} \exp\left[ig \int dx^+\, t^a\, \mathcal{A}_a^-(x^+, \mathbf{x}, 0)\right],
\end{aligned}$$

where T^a and t^a are the generators of $\mathfrak{su}(3)$ in fundamental and adjoint representations, respectively. With these we can calculate the inner product and one gets after three rounds of anticommutation and annihilation the result

$$\begin{aligned}
&\langle 0|\, a(x_2') d(x_1') b(x_0')\, \hat{S}_E\, b^\dagger(x_0) d^\dagger(x_1) a^\dagger(x_2)\,|0\rangle \\
&\quad = \mathcal{W}(x_0, B_0, \dots)(2\pi)^9 2^3 k_0^+ k_1^+ k_2^+ \left(\prod_{i=0}^{2} \delta\Big(k_i^+ - k_i^{\prime +}\Big) \delta^{(2)}(\mathbf{x}_i - \mathbf{x}_i')\right) \\
&\qquad \times \delta_{h_0, h_0'} \delta_{B_0, A_0'} \delta_{f, f_0'} \delta_{-h_0, h_1'} \delta_{B_1, A_1'} \delta_{f, f_1'} \delta_{\lambda_2, \lambda'} \delta_{b, a'}\, \langle 0|0\rangle\,.
\end{aligned} \tag{3.50}$$

Now the color factors in (3.48) can be separated using the result above, yielding

$$\begin{aligned}
&\sum_{\substack{A_0, A_1, a, \\ A_0', A_1', a' \\ B_0, B_1, b}} [U(\mathbf{x}_0)]_{B_0 A_0} \left[U^\dagger(\mathbf{x}_1)\right]_{A_1 B_1} [V(\mathbf{x}_2)]_{ba} \Big(T^{a'}\Big)^\dagger_{A_0' A_1'} (T^a)_{A_0 A_1} \delta_{B_0, A_0'} \delta_{B_1, A_1'} \delta_{b, a'} \\
&\quad = \sum_{a,b} [V(\mathbf{x}_2)]_{ba}\, \mathrm{tr}\big[U(\mathbf{x}_0) T^a U^\dagger(\mathbf{x}_1) T^b\big].
\end{aligned}$$

To calculate this, we need to know that the adjoint Wilson line $V(\mathbf{x})$ can be written element-wise as a trace:

$$[V(\mathbf{x})]_{ba} = 2\,\mathrm{tr}\left[U(\mathbf{x}) T^a U^\dagger(\mathbf{x}) T^b\right] \tag{3.51}$$

and the generator sum rule

$$\sum_a T^a_{AB} T^b_{CD} = \frac{1}{2}\left(\delta_{A,D}\delta_{B,C} - \frac{1}{N_c}\delta_{A,B}\delta_{C,D}\right). \tag{3.52}$$

Let us also define

$$S_{ij} := \frac{1}{N_c}\,\mathrm{tr}\left[U(\mathbf{x}_i)U^\dagger(\mathbf{x}_j)\right] \tag{3.53}$$

With these we get

$$\begin{aligned}\sum_{a,b}\left[V(\mathbf{x}_2)\right]_{ba}\mathrm{tr}\big[U(\mathbf{x}_0)T^aU^\dagger(\mathbf{x}_1)T^b\big] &= \frac{N_c^2}{2}\left[S_{02}S_{21}-\frac{1}{N_c^2}S_{01}\right]\\ &=: C,\end{aligned} \tag{3.54}$$

where, in addition to the relations (3.51), (3.52) and (3.53), the unitarity of the Wilson lines and the fact that $S_{22}=1$ were used.

Now we can plug the color factor (3.54) along with the rest of the inner product (3.50) back into (3.48) to get

$$\begin{aligned}&{}_{q\bar{q}g}\big\langle\gamma^*_{(T),L}\big|\,\hat{S}_E\,\big|\gamma^*_{(T),L}\big\rangle_{q\bar{q}g}\\ &= \left(\frac{eg}{4\pi}\right)^2\sum_{h_0,\lambda_2,(\lambda)}\sum_{h_0',\lambda_2',(\lambda')}\int\int dZdZ'\prod_{i=0}^{2}\left(\int\frac{d^2\mathbf{x}_i}{(2\pi)^2}\int\frac{d^2\mathbf{x}_i'}{(2\pi)^2}\right)\\ &\quad\times\Phi^*_{(T),L}(z_0',\dots)\Phi_{(T),L}(z_0,\dots)\times C\sum_f e_f\sum_{f'}e_{f'}\times(2\pi)^9 2^3 z_0z_1z_2\delta\left(z_0-z_0'\frac{q'^+}{q^+}\right)\\ &\quad\times\delta\left(z_1-z_1'\frac{q'^+}{q^+}\right)\delta\left(z_2-z_2'\frac{q'^+}{q^+}\right)\delta^{(2)}(\mathbf{x}_0-\mathbf{x}_0')\delta^{(2)}(\mathbf{x}_1-\mathbf{x}_1')\delta^{(2)}(\mathbf{x}_2-\mathbf{x}_2')\\ &\quad\times\delta_{h_0,h_0'}\delta_{f_0,f_0'}\delta_{f_1,f_1'}\delta_{\lambda_2,\lambda'}.\end{aligned} \tag{3.55}$$

Summing over the primed quantum numbers and integrating over the primed positions and primeless momentum fractions yields

$$\begin{aligned}&{}_{q\bar{q}g}\big\langle\gamma^*_{(T),L}\big|\,\hat{S}_E\,\big|\gamma^*_{(T),L}\big\rangle_{q\bar{q}g}\\ &= \left(\frac{eg}{4\pi}\right)^2 2^3(2\pi)^3\sum_{h_0,\lambda_2,(\lambda)}\int_0^1\int_0^1\int_0^1 dz_0'dz_1'\frac{dz_2'}{z_2'}\frac{q'^+}{q^+}\delta\left(\frac{q'^+}{q^+}(z_0'+z_1'+z_2')-1\right)\\ &\quad\times\delta(z_0'+z_1'+z_2'-1)\prod_{i=0}^{2}\left(\int\frac{d^2\mathbf{x}_i}{(2\pi)^2}\right)\Phi^*_{(T),L}(z_0',\mathbf{x}_0,\dots)\Phi_{(T),L}(z_0'\frac{q'^+}{q^+},\mathbf{x}_0,\dots)\\ &\quad\times C\sum_f e_f^2\end{aligned} \tag{3.56}$$

Lastly integrating over z_0', and writing the constants using the fine structure constant $\alpha_{em} = e^2/4\pi$ and $\bar{\alpha} := N_c g^2/4\pi^2$, we get

$$\begin{aligned}
&{}_{q\bar{q}g}\left\langle \gamma^*_{(T),L}\right| \hat{S}_E \left|\gamma^*_{(T),L}\right\rangle_{q\bar{q}g} \\
&= 2\pi\delta\left(\frac{q'^+}{q^+} - 1\right)\frac{2\alpha_{em}\bar{\alpha}N_c}{(2\pi)^2}\sum_f e_f^2 \int_0^1 dz_1 \int_0^{1-z_1}\frac{dz_2}{z_2} \\
&\quad\times \int\int\int d^2\mathbf{x}_0 d^2\mathbf{x}_1 \frac{d^2\mathbf{x}_2}{2\pi}\left[S_{02}S_{21} - \frac{1}{N_c^2}S_{01}\right] \\
&\quad\times \sum_{h_0,\lambda_2,(\lambda)} \left|\Phi_{(T),L}(x_0, x_1, x_2, 1-z_1-z_2, z_1, z_2, h_0, \lambda_2, (\lambda))\right|^2,
\end{aligned} \tag{3.57}$$

where we dropped the primes from the remaining momentum fractions. Note the new integration limit for z_2 which is due to the fact that a delta set $z_0 = 1 - z_1 - z_2$ and hence $1 - z_1 - z_2 \in [0, 1]$.

Lastly we need to calculate the NLO impact factors

$$\mathcal{I}_L^{q\bar{q}g}(x_0, x_1, x_2, 1-z_1-z_2, z_1, z_2) := \frac{1}{2}\sum_{h_0,\lambda_2} \left|\Phi_L(x_0, x_1, x_2, 1-z_1-z_2, z_1, z_2, h_0, \lambda_2)\right|^2 \tag{3.58}$$

$$\mathcal{I}_T^{q\bar{q}g}(x_0, x_1, x_2, 1-z_1-z_2, z_1, z_2) := \frac{1}{4}\sum_{h_0,\lambda_2,\lambda} \left|\Phi_T(x_0, x_1, x_2, 1-z_1-z_2, z_1, z_2, h_0, \lambda_2, \lambda)\right|^2, \tag{3.59}$$

for which we have to square the amplitudes (3.32) and (3.33). Just as with the LO impact factors (3.14) and (3.16) these definitions have the additional factor of $1/2$ and only the transverse polarization case has an actual average over the incoming state. For the polarization sums we will need the relations

$$\sum_\lambda \epsilon_\lambda^{i*}\epsilon_\lambda^j = \delta^{ij}$$
$$\sum_\lambda \lambda\epsilon_\lambda^{i*}\epsilon_\lambda^j = i\epsilon^{ij}$$

which directly imply

$$\sum_\lambda (\epsilon_\lambda^* \cdot x)(\epsilon_\lambda \cdot y) = x \cdot y \tag{3.60}$$

$$\sum_\lambda \lambda(\epsilon_\lambda^* \cdot x)(\epsilon_\lambda \cdot y) = i\epsilon^{ij}x_i y_j =: ix \wedge y, \tag{3.61}$$

where in the last equality the wedge product was defined.

Noting that linear terms in helicity h_0 cancel out when the helicity sum is carried out, and remembering that $h_0 = \pm 1/2,\ \lambda = \pm 1$, we can get the intermediate results

$$\sum_{h_0}\left[1-\frac{z_2}{1-z}\left(\frac{1\pm 2h_0\lambda_2}{2}\right)\right]^2 = 1+\left(1-\frac{z_2}{1-z}\right) =: 2P\left(\frac{z_2}{1-z}\right)$$

and

$$\sum_{h_0}\left[1-\frac{z_2}{1-z_1}\left(\frac{1-2h_0\lambda_2}{2}\right)\right]\left[1-\frac{z_2}{1-z_0}\left(\frac{1+2h_0\lambda_2}{2}\right)\right] = 2\left(1-\frac{1}{2}\frac{z_2}{1-z_1}-\frac{1}{2}\frac{z_2}{1-z_0}\right).$$

Using these, we get for the simpler longitudinal impact factor

$$\mathcal{I}_L^{q\bar{q}g}(\mathbf{x}_0,\mathbf{x}_1,\mathbf{x}_2,z_0,z_1,z_2) \tag{3.62}$$

$$\begin{aligned}
&= \frac{1}{2}\sum_{h_0,\lambda_2}(-4i^2)Q^2K_0^2(QX)\left\{z_1^2(1-z_1)^2\left[1-\frac{z_2}{1-z_1}\left(\frac{1-2h_0\lambda_2}{2}\right)\right]^2\frac{\epsilon^*_{\lambda_2}\cdot\mathbf{x}_{20}}{|\mathbf{x}_{20}|^2}\frac{\epsilon_{\lambda_2}\cdot\mathbf{x}_{20}}{|\mathbf{x}_{20}|^2}\right.\\
&\quad + z_0^2(1-z_0)^2\left[1-\frac{z_2}{1-z_0}\left(\frac{1+2h_0\lambda_2}{2}\right)\right]^2\frac{\epsilon^*_{\lambda_2}\cdot\mathbf{x}_{21}}{|\mathbf{x}_{21}|^2}\frac{\epsilon_{\lambda_2}\cdot\mathbf{x}_{21}}{|\mathbf{x}_{21}|^2} - z_0z_1(1\\
&\qquad - z_0)(1-z_1)\left[1-\frac{z_2}{1-z_1}\left(\frac{1-2h_0\lambda_2}{2}\right)\right]\left[1-\frac{z_2}{1-z_0}\left(\frac{1+2h_0\lambda_2}{2}\right)\right]\\
&\quad \left.\times\left\{\frac{\epsilon_{\lambda_2}\cdot\mathbf{x}_{20}}{|\mathbf{x}_{20}|^2}\frac{\epsilon^*_{\lambda_2}\cdot\mathbf{x}_{21}}{|\mathbf{x}_{21}|^2}+\frac{\epsilon^*_{\lambda_2}\cdot\mathbf{x}_{20}}{|\mathbf{x}_{20}|^2}\frac{\epsilon_{\lambda_2}\cdot\mathbf{x}_{21}}{|\mathbf{x}_{21}|^2}\right\}\right\}\\
&= 4Q^2K_0^2(QX)\left\{z_1^2(1-z_1)^2\frac{P\left(\frac{z_2}{1-z_1}\right)}{|\mathbf{x}_{20}|^2}+z_0^2(1-z_0)^2\frac{P\left(\frac{z_2}{1-z_0}\right)}{|\mathbf{x}_{21}|^2}\right.\\
&\qquad \left.-2z_0z_1(1-z_0)(1-z_1)\left[1-\frac{1}{2}\left(\frac{z_2}{1-z_1}+\frac{z_2}{1-z_0}\right)\right]\frac{\mathbf{x}_{20}\cdot\mathbf{x}_{21}}{|\mathbf{x}_{20}|^2|\mathbf{x}_{21}|^2}\right\}
\end{aligned}$$

Squaring the transverse amplitude (3.32) is a similar, however more cumbersome operation. We'll need some intermediate results: the following helicity sums

$$\sum_{h_0}[1-2z\pm 2h_0\lambda]^2\left[1-\frac{z_2}{1-z}\left(\frac{1\mp 2h_0\lambda_2}{2}\right)\right]^2 = 4\left[z^2+(1-z)^2\right]P\left(\frac{z_2}{1-z}\right),$$

$$\sum_{h_0,\lambda_2,\lambda}\delta_{\lambda,\lambda_2}\left[\frac{\delta_{\lambda,-2h_0}}{(1-z_1)^2}+\frac{\delta_{\lambda,2h_0}}{(1-z_0)^2}\right]=2\left[\frac{1}{(1-z_1)^2}+\frac{1}{(1-z_0)^2}\right],$$

and

$$\sum_{h_0}[1-2z_1+2h_0\lambda][1-2z_0-2h_0\lambda]\left[1-\frac{z_2}{1-z_1}\left(\frac{1-2h_0\lambda_2}{2}\right)\right]\left[1-\frac{z_2}{1-z_0}\left(\frac{1+2h_0\lambda_2}{2}\right)\right]$$
$$=-4[z_1(1-z_0)+z_0(1-z_1)]\left(1-\frac{1}{2}\left(\frac{z_2}{1-z_1}+\frac{z_2}{1-z_0}\right)\right)+2\lambda\lambda_2\frac{z_2(z_1-z_0)^2}{(1-z_1)(1-z_0)}.$$

In the interference term of the two delayed gluon emissions one sees the following polarization sums

$$\sum_{\lambda,\lambda_2}\left\{\left(\epsilon^*_\lambda\cdot X^{10}_{20}\right)\left(\epsilon_\lambda\cdot X^{01}_{21}\right)\left(\epsilon^*_{\lambda_2}\cdot\frac{\mathbf{x}_{21}}{|\mathbf{x}_{21}|}\right)\left(\epsilon_{\lambda_2}\cdot\frac{\mathbf{x}_{20}}{|\mathbf{x}_{20}|}\right)+h.c.\right\}$$
$$=2\left(X^{10}_{20}\cdot X^{01}_{21}\right)\frac{\mathbf{x}_{20}\cdot\mathbf{x}_{21}}{|\mathbf{x}_{20}|^2|\mathbf{x}_{21}|^2}$$

and

$$\sum_{\lambda,\lambda_2}\lambda\lambda_2\left\{\left(\epsilon^*_\lambda\cdot X^{10}_{20}\right)\left(\epsilon_\lambda\cdot X^{01}_{21}\right)\left(\epsilon^*_{\lambda_2}\cdot\frac{\mathbf{x}_{21}}{|\mathbf{x}_{21}|}\right)\left(\epsilon_{\lambda_2}\cdot\frac{\mathbf{x}_{20}}{|\mathbf{x}_{20}|}\right)+h.c.\right\}$$
$$=\frac{-2z_2}{(1-z_1)(1-z_0)}\frac{(\mathbf{x}_{20}\wedge\mathbf{x}_{21})^2}{|\mathbf{x}_{20}|^2|\mathbf{x}_{21}|^2},$$

where the shorthand $X^{ij}_{mn}:=\mathbf{x}_{ij}-\frac{z_2}{1-z_i}\mathbf{x}_{mn}$ was defined. And lastly for the interference terms between a delayed and instant emission

$$\sum_{\lambda,h_0}[1-2z_1+2h_0\lambda]\left[1-\frac{z_2}{1-z_1}\left(\frac{1-2h_0\lambda_2}{2}\right)\right]\delta_{\lambda,\lambda_2}\left[\frac{\delta_{\lambda,-2h_0}}{1-z_1}-\frac{\delta_{\lambda,2h_0}}{1-z_0}\right]$$
$$=-\left(\frac{2z_1z_0}{(1-z_1)^2}+\frac{2(1-z_1)}{1-z_0}\right)$$

and

$$\sum_{\lambda,h_0}[1-2z_0-2h_0\lambda]\left[1-\frac{z_2}{1-z_0}\left(\frac{1+2h_0\lambda_2}{2}\right)\right]\delta_{\lambda,\lambda_2}\left[\frac{\delta_{\lambda,-2h_0}}{1-z_1}-\frac{\delta_{\lambda,2h_0}}{1-z_0}\right]$$
$$=\left(\frac{2(1-z_0)}{1-z_1}+\frac{2z_1z_0}{(1-z_0)^2}\right).$$

With these intermediate results one can simplify the squared amplitude (3.32) to get

$$
\begin{aligned}
&\mathcal{I}_T^{q\bar{q}g}(\mathbf{x}_0,\mathbf{x}_1,\mathbf{x}_2,z_0,z_1,z_2)\\
&= \left[\frac{QXK_1(QX)}{X^2}\right]^2 \Bigg\{ z_1^2(1-z_1)^2\left[z_1^2+(1-z_1)^2\right]\frac{P\left(\frac{z_2}{1-z_1}\right)}{|\mathbf{x}_{20}|^2}\left(\mathbf{x}_{10}-\frac{z_2}{1-z_1}\mathbf{x}_{20}\right)^2\\
&\quad + z_0^2(1-z_0)^2\left[z_0^2+(1-z_0)^2\right]\frac{P\left(\frac{z_2}{1-z_0}\right)}{|\mathbf{x}_{21}|^2}\left(\mathbf{x}_{01}-\frac{z_2}{1-z_0}\mathbf{x}_{21}\right)^2\\
&\quad + \frac{z_0^2z_1^2z_2^2}{2}\left[\frac{1}{(1-z_1)^2}+\frac{1}{(1-z_0)^2}\right]\\
&\quad + 2z_1(1-z_1)z_0(1-z_0)[z_1(1-z_0)+z_0(1-z_1)]\left[1-\frac{1}{2}\left(\frac{z_2}{1-z_1}+\frac{z_2}{1-z_0}\right)\right]\\
&\quad \times\left(\mathbf{x}_{10}-\frac{1}{(1-z_1)^2}\mathbf{x}_{20}\right)\cdot\left(\mathbf{x}_{01}-\frac{1}{(1-z_0)^2}\mathbf{x}_{21}\right)\frac{\mathbf{x}_{20}\cdot\mathbf{x}_{21}}{|\mathbf{x}_{20}|^2|\mathbf{x}_{21}|^2}\\
&\quad + z_0z_1z_2^2\frac{(z_1-z_0)^2}{(1-z_1)(1-z_0)}\frac{(\mathbf{x}_{20}\wedge\mathbf{x}_{21})^2}{|\mathbf{x}_{20}|^2|\mathbf{x}_{21}|^2}\\
&\quad + z_0z_1^2z_2\left[\frac{z_1z_0}{1-z_1}+\frac{(1-z_1)^2}{1-z_0}\right]\left(\mathbf{x}_{10}-\frac{1}{(1-z_1)^2}\mathbf{x}_{20}\right)\cdot\frac{\mathbf{x}_{20}}{|\mathbf{x}_{20}|^2}\\
&\quad + z_0^2z_1z_2\left[\frac{(1-z_0)^2}{1-z_1}+\frac{z_1z_0}{1-z_0}\right]\left(\mathbf{x}_{01}-\frac{1}{(1-z_0)^2}\mathbf{x}_{21}\right)\cdot\frac{\mathbf{x}_{21}}{|\mathbf{x}_{21}|^2}\Bigg\},
\end{aligned}
\tag{3.63}
$$

where the first and second terms are the squares of the two delayed emission graphs, the third is the square of the instant graphs, the fourth and fifth are from the interference of the delayed graphs and the last two are from the interferences between the delayed and instant emissions.

Lastly we need to work around the lack of the correct loop diagram contribu-

tion. As a place holder (p.h.) we will use the result from [3]:

$$
\begin{aligned}
&{}_{q\bar{q}}\Big\langle \gamma^*_{(T),L}\Big(q^{'+}\Big)\Big|\,\hat{S}_E\,\Big|\gamma^*_{(T),L}\Big(q^{+}\Big)\Big\rangle^{p.h.}_{q\bar{q}} \\
&= 2\pi\delta\Big(\frac{q^{'+}}{q^+}-1\Big)\frac{2N_c\alpha_{em}}{(2\pi)^2}\sum_f e_f^2\int d\mathbf{x}_0\int d\mathbf{x}_1\int_0^1 dz_1 S_{01}[\mathcal{A}]\,\Big\{\mathcal{I}^{LO}_{T,L}(\mathbf{x}_0,\mathbf{x}_1,z_0,z_1) \\
&\qquad -\Big(1-\frac{1}{N_c^2}\Big)\bar{\alpha}\int_0^{1-z_1}\frac{dz_2}{z_2}\int\frac{d^2\mathbf{x}_2}{2\pi}\,\mathcal{I}^{q\bar{q}g}_{T,L}(\mathbf{x}_0,\mathbf{x}_1,\mathbf{x}_2,z_0,z_1,z_2)\Big\}\,.
\end{aligned}
\tag{3.64}
$$

We write the true $q\bar{q}$ result into a correction term to (3.64):

$$
\begin{aligned}
&{}_{q\bar{q}}\Big\langle \gamma^*_{(T),L}\Big(q^{'+}\Big)\Big|\,\hat{S}_E\,\Big|\gamma^*_{(T),L}\Big(q^{+}\Big)\Big\rangle_{q\bar{q}} \\
&= {}_{q\bar{q}}\Big\langle \gamma^*_{(T),L}\Big(q^{'+}\Big)\Big|\,\hat{S}_E\,\Big|\gamma^*_{(T),L}\Big(q^{+}\Big)\Big\rangle^{p.h.}_{q\bar{q}} \\
&- {}_{q\bar{q}}\Big\langle \gamma^*_{(T),L}\Big(q^{'+}\Big)\Big|\,\hat{S}_E\,\Big|\gamma^*_{(T),L}\Big(q^{+}\Big)\Big\rangle^{p.h.}_{q\bar{q}} + {}_{q\bar{q}}\Big\langle \gamma^*_{(T),L}\Big(q^{'+}\Big)\Big|\,\hat{S}_E\,\Big|\gamma^*_{(T),L}\Big(q^{+}\Big)\Big\rangle_{q\bar{q}} \\
&=: {}_{q\bar{q}}\Big\langle \gamma^*_{(T),L}\Big(q^{'+}\Big)\Big|\,\hat{S}_E\,\Big|\gamma^*_{(T),L}\Big(q^{+}\Big)\Big\rangle^{p.h.}_{q\bar{q}} + \Delta^{q\bar{q}},
\end{aligned}
\tag{3.65}
$$

where a name $\Delta^{q\bar{q}}$ was defined for the correction term. We will denote the impact factors associated with the correction term $\Delta^{q\bar{q}}$ by $\mathcal{I}^{q\bar{q}}_{T,L}$.

Now we can combine the LO and real NLO contributions (3.47) and (3.57), and the placeholder virtual pieces (3.64) and (3.65), in the equation (3.40) and simplify to get the cross section:

$$
\begin{aligned}
\sigma^{\gamma}_{T,L}[\mathcal{A}] &= 2\frac{2N_c\alpha_{em}}{(2\pi)^2}\sum_f e_f^2\int d^2\mathbf{x}_0\int d^2\mathbf{x}_1\int_0^1 dz_1 \\
&\times\Big\{[1-S_{01}[\mathcal{A}]]\mathcal{I}^{LO}_{T,L}(\mathbf{x}_0,\mathbf{x}_1,1-z_1,z_1) - S_{01}[\mathcal{A}]\mathcal{I}^{q\bar{q}}_{T,L}(\mathbf{x}_0,\mathbf{x}_1,z_1) \\
&+\bar{\alpha}\int\frac{d^2\mathbf{x}_2}{2\pi}\int_0^{1-z_1}\frac{dz_2}{z_2}[S_{01}[\mathcal{A}]-S_{02}[\mathcal{A}]S_{21}[\mathcal{A}]]\;\mathcal{I}^{q\bar{q}g}_{T,L}(\mathbf{x}_0,\mathbf{x}_1,\mathbf{x}_2,z_0,z_1,z_2)\Big\}\,,
\end{aligned}
\tag{3.66}
$$

where the additional factor of two comes from the choice of the impact factor definitions. Without the introduced correction term this is the same result as in [3]. The fact that the term inversely proportional to N_c^{-2} cancels between the real

and virtual contributions is not a coincidence as the virtual part was derived using the LO and real NLO results.

The result (3.66) is now the generalization of the leading order dipole factorization that was discussed in Chapter 2. The leading order $q\bar{q}$ scattering term neatly gets a correction due to the existence of the internal loops at this order and additionally there is now a scattering term where instead of the single dipole scattering there is now the $q\bar{q}g$ triplet scattering represented by two dipoles. Also at this order the QED/QCD photon splittings and the QCD scattering are factorized into separate terms just like at leading order.

Note where the so far unknown $\mathcal{I}^{q\bar{q}}$ correction term was written in (3.66) as it uses some information about the scattering process specific to the NLO $q\bar{q}$ process. Firstly, this process will have the same Wilson line structure as the LO scattering since the gluon in the internal loop does not take part in the scattering and thus only the quark and antiquark will go through the color rotation by the Wilson line. Hence it is written alongside the leading order impact factor. Secondly, in the computation of the impact factor the gluon loop is integrated over so the result can with the constraining conservation of momentum only depend on one of the fractional quark momenta, and the quark positions $\mathbf{x}_0$ and $\mathbf{x}_1$. Lastly, by vertex considerations, the NLO $q\bar{q}$ contribution will contain terms of the order of α_{em} and $\alpha_{em}\alpha_s$ so in this notation the impact factor-like term $\mathcal{I}^{q\bar{q}}_{T,L}$ will contain a section proportional to α_s, unlike the LO and $q\bar{q}g$ impact factors. The NLO $q\bar{q}$ light cone wavefunction relevant to this has been calculated in [10] where the result agrees with these deductions.

The reader might have noticed that the integrals over the NLO impact factors are not wholly convergent as there are singularities as $\mathbf{x}_2 \to \mathbf{x}_0$, $\mathbf{x}_2 \to \mathbf{x}_1$ and $z_2 \to 0$ in the $q\bar{q}g$ impact factor. This was not brought up as it turned out that in the evaluation of the cross section the integrals get introduced additional kernels in the form of the dipole correlators S_{ij}, which behave in a fortunate way due to color transparency:

$$1 - S_{ij}[\mathcal{A}] \propto |\mathbf{x}_i - \mathbf{x}_j|^2, \text{ as } \mathbf{x}_j \to \mathbf{x}_i, \tag{3.67}$$

which nicely nullifies the divergent singularities at the limits where the emitted

gluon is arbitrarily close to one of the quarks. In other words the color transparency states that at the soft gluon emission limit, the qg or $\bar{q}g$ pairs behave as color dipoles with small radii whose interaction cross section is proportional to the dipole size squared, which counteracts the soft gluon divergence in the photon splitting amplitude. We are then left with the unregulated logarithmic z_2 divergence in the $q\bar{q}g$ contribution that we will look at in the next section.

Note that the NLO $q\bar{q}$ contribution written in the form in (3.66) does not have this soft z_2 divergence and so it does not affect the discussion of the next section. This can be said a priori since the process has been calculated at $z_2 \to 0$ limit in the derivation of the Balitsky-Kovchegov equation [11] and the result agrees with the soft divergence part obtained here. Thus the soft divergence in the loop calculations can be done in the same fashion as is done in the next chapter leading to the same result as here. In other words the $q\bar{q}$ contribution contains the same divergence that we regulate here and no further divergence. This deduction relies on the fact that the calculations done in [11] do not rely on a state unitarity argument and since the divergence is the same, the mistake done with the unitarity argument in [3] does not change the behavior on the $z_2 \to 0$ limit.

3.5 Regularization of the NLO cross section soft divergence

We have now calculated the polarized cross sections (3.66), but they are divergent as $z_2 \to 0$, which we need to resolve. This so-called rapidity divergence of the polarized cross sections stems from the photon splitting amplitudes calculated in Section 3.2 which are logarithmically divergent in z_2.

One way to handle this is to consider all gluons in the system parallel to the incoming photon as part of the projectile and all antiparallel ones as part of the target [12]. One can then introduce a cut-off k_f^+ in k_2^+, such that the emitted gluons taken into consideration have their momentum bound from below by a non-zero quantity.

The existence of such a cut-off seems reasonable as the interaction takes a finite time and one can see that an emitted gluon with arbitrarily small momentum in the frame does not have a sufficient lifetime to interact with the target [13]. Another way to look at this is to consider the rapidity of the emitted gluon, which is proportional to $\log(1/z_2)$, which implies that the soft gluon has high negative rapidity. In the soft limit $z_2 \to 0$ the rapidity then goes to $-\infty$ and the emitted gluon becomes collinear with the target which has rapidity near $-\infty$ [14]. Hence it is appropriate to absorb the soft gluon into the target according to its movement direction. It is also to be expected that this cut-off is scale dependent. Thus we have for the limits $z_f \leq z_2 \leq 1 - z_1$ for the gluon fractional momentum, where $z_f \coloneqq k_f^+/q^+$.

So we begin the regularization by setting the lower integration limit of z_2 in (3.66) to z_f, and introduce the following term:

$$\begin{aligned}\Delta\mathcal{I}_{T,L}^{q\bar{q}g}(\mathbf{x}_0, \mathbf{x}_1, \mathbf{x}_2, z_0, z_1, z_2) \coloneqq &\mathcal{I}_{T,L}^{q\bar{q}g}(\mathbf{x}_0, \mathbf{x}_1, \mathbf{x}_2, z_0, z_1, z_2) \\ &- \mathcal{I}_{T,L}^{q\bar{q}g}(\mathbf{x}_0, \mathbf{x}_1, \mathbf{x}_2, z_0, z_1, 0). \end{aligned} \tag{3.68}$$

Looking at the equations (3.62) and (3.63) one sees immediately that they simplify quite a bit at $z_2 = 0$ and in fact one gets

$$\mathcal{I}_{T,L}^{q\bar{q}g}(\mathbf{x}_0, \mathbf{x}_1, \mathbf{x}_2, z_0, z_1, 0) = \frac{\mathbf{x}_{01}^2}{\mathbf{x}_{02}^2 \mathbf{x}_{21}^2} \mathcal{I}_{T,L}^{LO}(\mathbf{x}_0, \mathbf{x}_1, z_0, z_1). \tag{3.69}$$

Lastly before we can continue, we must take care of the Color Glass Condensate

(CGC) model averaging over the target gluon field $\mathcal{A}$. This means that we neglect the quantum mechanical fluctuations in the properties of the target color field $\mathcal{A}$ and study the average behavior of the system in the scattering. In practice this is done by replacing the dipole correlators S_{ij} with their implicit expectation values for a given cut-off:

$$S_{ij}[\mathcal{A}] \to \langle S_{ij} \rangle_{z_f},$$

where the subscript z_f denotes that the expectation value is a function of the cut-off, which it certainly is as the cut-off dictates how many additional particles we associate with the target.

With these we can write the cross sections (3.66), neglecting the virtual $q\bar{q}$ contribution term, as

$$\begin{aligned}\sigma^{\gamma}_{T,L} = 2\frac{2N_c\alpha_{em}}{(2\pi)^2}\sum_f e_f^2 \int d^2\mathbf{x}_0 \int d^2\mathbf{x}_1 \int_0^1 dz_1 \times \Bigg\{ \big[1 - \langle S_{01}\rangle_{z_f}\big]\mathcal{I}^{LO}_{T,L}(\mathbf{x}_0, \mathbf{x}_1, 1-z_1, z_1) \\ + \bar{\alpha}\int \frac{d^2\mathbf{x}_2}{2\pi}\int_{z_f}^{1-z_1}\frac{dz_2}{z_2}\langle S_{01} - S_{02}S_{21}\rangle_{z_f}\, \Delta\mathcal{I}^{q\bar{q}g}_{T,L}(\mathbf{x}_0, \mathbf{x}_1, \mathbf{x}_2, 1-z_1, z_1, z_2) \\ + \bar{\alpha}\int \frac{d^2\mathbf{x}_2}{2\pi}\int_{z_f}^{1-z_1}\frac{dz_2}{z_2}\langle S_{01} - S_{02}S_{21}\rangle_{z_f}\, \frac{\mathbf{x}_{01}^2}{\mathbf{x}_{02}^2\mathbf{x}_{21}^2}\mathcal{I}^{LO}_{T,L}(\mathbf{x}_0, \mathbf{x}_1, 1-z_1, z_1)\Bigg\},\end{aligned}$$

where now the last line's integrand is z_2 independent and the logarithmic integral can be performed to get, after a rearrangement

$$\begin{aligned}\sigma^{\gamma}_{T,L} = 2\frac{2N_c\alpha_{em}}{(2\pi)^2}\sum_f e_f^2 \int d^2\mathbf{x}_0 \int d^2\mathbf{x}_1 \int_0^1 dz_1 \Bigg\{ \Bigg[1 - \langle S_{01}\rangle_{z_f} \\ + \bar{\alpha}\log\left(\frac{1-z_1}{z_f}\right)\int \frac{d^2\mathbf{x}_2}{2\pi}\frac{\mathbf{x}_{01}^2}{\mathbf{x}_{02}^2\mathbf{x}_{21}^2}\langle S_{01} - S_{02}S_{21}\rangle_{z_f}\Bigg]\mathcal{I}^{LO}_{T,L}(\mathbf{x}_0, \mathbf{x}_1, 1-z_1, z_1) \\ + \bar{\alpha}\int \frac{d^2\mathbf{x}_2}{2\pi}\int_{z_f}^{1-z_1}\frac{dz_2}{z_2}\langle S_{01} - S_{02}S_{21}\rangle_{z_f}\, \Delta\mathcal{I}^{q\bar{q}g}_{T,L}(\mathbf{x}_0, \mathbf{x}_1, \mathbf{x}_2, 1-z_1, z_1, z_2)\Bigg\}.\end{aligned} \tag{3.70}$$

Here we are still left with a cross section that depends explicitly on the cut-off, which certainly cannot stand. Should this be a workable regularization, we must arrive at a result that is independent of the choice of cut-off, i.e.

$$\frac{\partial}{\partial z_f}\sigma^{\gamma}_{T,L}\big(q^+, Q^2\big) = 0.$$

However, the cross section (3.70) depends on the logarithm of the cut-off, so we'll get a more convenient result when we impose the equivalent requirement that

$$\frac{\partial}{\partial \log z_f}\sigma_{T,L}^{\gamma}\big(q^+, Q^2\big) = 0.$$

Applying this condition to equation (3.70) we get

$$\begin{aligned} 0 = \frac{\partial}{\partial \log z_f}\Big\{&\mathcal{I}_{T,L}^{LO}(\mathbf{x}_0, \mathbf{x}_1, 1-z_1, z_1) \\ &\times \left[1 - \langle S_{01}\rangle_{z_f} + \bar{\alpha}\log\left(\frac{1-z_1}{z_f}\right)\int \frac{d^2\mathbf{x}_2}{2\pi}\frac{\mathbf{x}_{01}^2}{\mathbf{x}_{02}^2\mathbf{x}_{21}^2}\langle S_{01} - S_{02}S_{21}\rangle_{z_f}\right]\Big\} \\ &+ \frac{\partial}{\partial \log z_f}\bar{\alpha}\int\frac{d^2\mathbf{x}_2}{2\pi}\int_{z_f}^{1-z_1}\frac{dz_2}{z_2}\langle S_{01} - S_{02}S_{21}\rangle_{z_f}\Delta\mathcal{I}_{T,L}^{q\bar{q}g}(\mathbf{x}_0, \mathbf{x}_1, \mathbf{x}_2, 1-z_1, z_1, z_2). \end{aligned} \tag{3.71}$$

This is satisfied to the first order in $\bar{\alpha}$ when one sets

$$\frac{\partial}{\partial \log z_f}\langle S_{01}\rangle_{z_f} = \bar{\alpha}\int\frac{d^2\mathbf{x}_2}{2\pi}\frac{\mathbf{x}_{01}^2}{\mathbf{x}_{02}^2\mathbf{x}_{21}^2}\langle S_{02}S_{21} - S_{01}\rangle_{z_f}, \tag{3.72}$$

which is an evolution equation of the quark-antiquark dipole correlator. This choice causes the remaining contributions to $\langle S_{01}\rangle_{z_f}$ in the equation (3.71) become at least of degree $\bar{\alpha}^2$ or higher.

With the evolution equation (3.72) we can renormalize the cross section by absorbing the cut-off dependence into the evolution equation and defining a regularized dipole correlator:

$$\langle S_{01}\rangle^r \coloneqq \langle S_{01}\rangle_{z_f} + \bar{\alpha}\log z_f\int\frac{d^2\mathbf{x}_2}{2\pi}\frac{\mathbf{x}_{01}^2}{\mathbf{x}_{02}^2\mathbf{x}_{21}^2}\big(\langle S_{02}S_{21} - S_{01}\rangle_{z_f}\big) \tag{3.73}$$

$$\approx \langle S_{01}\rangle_{z_f} + \bar{\alpha}\log z_f\int\frac{d^2\mathbf{x}_2}{2\pi}\frac{\mathbf{x}_{01}^2}{\mathbf{x}_{02}^2\mathbf{x}_{21}^2}\big(\langle S_{02}\rangle_{z_f}\langle S_{21}\rangle_{z_f} - \langle S_{01}\rangle_{z_f}\big), \tag{3.74}$$

where in the approximation the correlations between the dipoles were neglected, i.e. $\langle S_{02}S_{21}\rangle_{z_f} \approx \langle S_{02}\rangle_{z_f}\langle S_{21}\rangle_{z_f}$. With this we can finally write the regularized cross section

$$\sigma_{T,L}^{\gamma} = 2\frac{2N_c\alpha_{em}}{(2\pi)^2}\sum_f e_f^2\int d^2\mathbf{x}_0\int d^2\mathbf{x}_1\int_0^1 dz_1\Big\{\Big[1 - \langle S_{01}\rangle^r \tag{3.75}$$

$$+\,\bar{\alpha}\log(1-z_1)\int\frac{d^2\mathbf{x}_2}{2\pi}\frac{\mathbf{x}_{01}^2}{\mathbf{x}_{02}^2\mathbf{x}_{21}^2}(\langle S_{01}\rangle^r-\langle S_{02}\rangle^r\langle S_{21}\rangle^r)\Big]\,\mathcal{I}_{T,L}^{LO}(\mathbf{x}_0,\mathbf{x}_1,1-z_1,z_1)$$
$$+\,\bar{\alpha}\int\frac{d^2\mathbf{x}_2}{2\pi}\int_0^{1-z_1}\frac{dz_2}{z_2}(\langle S_{01}\rangle^r-\langle S_{02}\rangle^r\langle S_{21}\rangle^r)\;\Delta\mathcal{I}_{T,L}^{q\bar{q}g}(\mathbf{x}_0,\mathbf{x}_1,\mathbf{x}_2,1-z_1,z_1,z_2)\Big\},$$

where the error we make when substituting the regularized dipole correlator (3.74) is of the order of $\bar{\alpha}^2$, i.e. a NNLO contribution, so we may neglect it here. Since the divergence is now regulated the lower limit of the gluon fractional momentum integral was set back to zero.

We now have arrived at regularized polarized cross sections that do not diverge. However, before we can move on to evaluate these cross sections we still need to answer an unresolved question – how do we get the dipole correlator $\langle S_{ij}\rangle$ from the equation (3.72), or otherwise. Finding the answer to this question is the purpose of the next section.

3.6 Solutions for the quark dipole correlator $\langle S_{ij}\rangle$

The last piece we need to be able to compute the cross sections are the dipole correlators $\langle S_{ij}\rangle$ and $\langle S_{ij}S_{jk}\rangle$ that encode the interactions of a quark-antiquark pair and two pairs, respectively. The non-perturbative dense soft gluon section of the system described by the CGC model was woven into these dipole correlators by using the eikonal scattering approximation, which essentially gave us that the dipole correlators stem from the Wilson lines of the quarks, which were path ordered integrals in the gluon field. However, in light of the work done in the regularization Section 3.5, instead of studying the dipole correlators in this fine detail, we can use the dynamical consistency equations that we found to solve the dipole correlators. Via these evolution equations we can simultaneously get a description of the quark-antiquark dipole interactions and regulate the soft divergence.

The first consistency equation found in the previous section is the evolution equation (3.72):

$$\frac{\partial}{\partial\log z_f}\langle S_{01}\rangle_{z_f}=\bar{\alpha}\int\frac{d^2\mathbf{x}_2}{2\pi}\frac{\mathbf{x}_{01}^2}{\mathbf{x}_{02}^2\mathbf{x}_{21}^2}\langle S_{02}S_{21}-S_{01}\rangle_{z_f},$$

which is a part of the full JIMWLK evolution equation for the whole probability density. From the JIMWLK equation one could solve for correlators of S_{ij} of arbitrary order [5]. This is our first opportunity to try to solve the dipole correlator which would need to be done numerically as it has resisted analytical solution efforts. However, as this is not a closed equation, solving it numerically is a challenging task and while it has been done [15–17], implementing it here is out of scope.

At the limit of large N_c the higher order moments between the two coupled dipole correlators, representing pairwise interactions in the quark-antiquark-gluon set, die off decoupling the equation (3.72) into a closed equation for the single quark-antiquark correlator known as the Balitsky–Kovchegov (BK) equation:

$$\frac{\partial}{\partial \log z_f}\langle S_{01}\rangle_{z_f} = \bar{\alpha}\int \frac{d^2\mathbf{x}_2}{2\pi}\frac{\mathbf{x}_{01}^2}{\mathbf{x}_{02}^2\mathbf{x}_{21}^2}\big(\langle S_{02}\rangle_{z_f}\langle S_{21}\rangle_{z_f} - \langle S_{01}\rangle_{z_f}\big).$$

The numerical solution of the BK equation has been studied extensively [18–26], and it has turned out [15, 17] that as an approximation the BK equation is a surprisingly good at capturing the dynamics described by the JIMWLK equation. In the study [17] by Kovchegov et al. they found that the relative disagreement between the JIMWLK and BK equations was two orders of magnitude smaller that one would expect by a simple $1/N_c$ expansion approximation: the difference was found to be around 0.1% instead of $1/N_c^2 \approx 11\%$. The relative ease of use and the quality of the approximation of the BK equation has led to its popularity over the JIMWLK equation. In recent years work has been done towards an NLO BK equation [27–31]. The regularized cross sections (3.75) were already written using the BK equation since we neglected the correlations in equation (3.74).

Neither of the evolution equations discussed above are simple to implement numerically, especially so with the JIMWLK equation. Prior to the advancements made on the numerical solution of either of the equations, a fairly good phenomenological model was found by Golec-Biernat and Wüsthoff [32] that described DIS data fairly well at the time at small x: $x \leq 10^{-2}$ [33]. To get some initial qualitative results for the NLO corrections, in this work we opt to use the phenomenological model found by Golec-Biernat and Wüsthoff (GBW) for the dipole cross section.

In the GBW model the dipole cross section is

$$S_{GBW}(r) = \sigma_0 e^{-r^2 Q_s^2/4}, \tag{3.76}$$

where the scale Q_s is x dependent: $Q_s(x)^2 = Q_0(x_0/x)^\lambda$ and where σ_0, x_0 and λ are fit parameters. To apply this we need to understand where the fit parameter σ_0 arises. This is connected to a seemingly superfluous planar integration that is left over after the change of integration variables done in Section 4. Specifically the integration over the parameter $\mathbf{b} = (\mathbf{x}_1 + \mathbf{x}_2)/2$. In the choice of the GBW dipole cross section we have neglected the finite size of the target, and we need to additionally at least introduce a simple step function to give a crude description of the size of the target:

$$2\int d^2\mathbf{b} S(\mathbf{r}, \mathbf{b}) \approx S(\mathbf{r}) \cdot 2\int_{target} d^2\mathbf{b} \equiv S_{GBW}(\mathbf{r}) =: S(\mathbf{r}),$$

where at the triple bar the quantity is identified as the GBW dipole cross section, which then is renamed at the last equality.

We now have the last piece required for the computation of the regularized polarized cross sections (3.75) so we may continue into a numerical study in Section 4 to see what kind of contribution these next-to-leading order corrections yield to the leading order results.

Chapter 4

Numerical evaluation of the next-to-leading order cross sections and DIS structure functions

In this chapter the procedure to evaluate the cross sections is elaborated on. This entails transforming the integral to a slightly more manageable form by parameterizing the integrand by the dimensions of the dipole-gluon system and modeling of the dipole correlators $\langle S_{01} \rangle$ and $\langle S_{01} - S_{20}S_{21} \rangle$ with the GBW model discussed in the Section 3.6. Lastly we will need to implement some form of the QCD running coupling for α_s.

First the re-parameterization of the integrand, which only depends on the relative distances between the particles, not on the positions of the particles themselves. Considering this, a good choice turns out to be:

$$\begin{aligned} \mathbf{r} &\coloneqq \mathbf{x}_0 - \mathbf{x}_1, \\ \mathbf{b} &\coloneqq \frac{\mathbf{x}_0 + \mathbf{x}_1}{2}, \\ \mathbf{z} &\coloneqq \mathbf{x}_2 - \mathbf{b}. \end{aligned}$$

Geometrically these variables represent the size of the quark-antiquark dipole, the

average position of the quark-antiquark system and the distance of the gluon from this 'center' of the dipole, respectively. The Jacobian determinant of this change of variables is nicely unity.

With this change of variables and the application of the GBW dipole cross section model (3.76) from the Section 3.6, the cross section (3.75) becomes

$$\begin{aligned}\sigma^{\gamma}_{T,L}(q^+,Q^2) = 2\frac{2N_c\alpha_{em}}{(2\pi)^2}\sigma_0\sum_f e_f^2\int d^2\mathbf{r}\int_0^1 dz_1\Bigg\{\Bigg[1-S(\mathbf{r})+\bar{\alpha}\log\left(1-z_1\right)\\ \times\int\frac{d^2\mathbf{z}}{2\pi}\frac{\mathbf{r}^2}{\left(\frac{\mathbf{r}}{2}-\mathbf{z}\right)^2\left(\frac{\mathbf{r}}{2}+\mathbf{z}\right)^2}\Big(S(\mathbf{r})-S\Big(\frac{\mathbf{r}}{2}-\mathbf{z}\Big)S\Big(\frac{\mathbf{r}}{2}+\mathbf{z}\Big)\Big)\Bigg]\mathcal{I}^{LO}_{T,L}(\mathbf{r},1-z_1,z_1)\\ +\bar{\alpha}\int\frac{d^2\mathbf{z}}{2\pi}\int_0^{1-z_1}\frac{dz_2}{z_2}\Big(S(\mathbf{r})-S\Big(\frac{\mathbf{r}}{2}-\mathbf{z}\Big)S\Big(\frac{\mathbf{r}}{2}+\mathbf{z}\Big)\Big)\,\Delta\mathcal{I}^{q\bar{q}g}_{T,L}(\mathbf{r},\mathbf{z},z_1,z_2)\Bigg\}.\end{aligned} \tag{4.1}$$

Three models of varying complexity of the QCD running coupling were used:

$$\begin{aligned}\alpha_s &= 0.2,\\ \alpha_s(Q^2) &= \frac{12\pi}{(33-2N_f)\log\left(\frac{Q^2}{\Lambda^2_{QCD}}\right)},\\ \alpha_s(\mathbf{x}_{01}^2,\mathbf{x}_{20}^2,\mathbf{x}_{21}^2) &= \alpha_s\left(Q^2=\frac{4e^{-2\gamma_E}}{\min(\mathbf{x}_{01}^2,\mathbf{x}_{20}^2,\mathbf{x}_{21}^2)}\right).\end{aligned} \tag{4.2}$$

The first, constant coupling, only gives a rough relative scaling for the LO and NLO contributions that is in the rough ballpark for the Q^2 range we are interested in, and was used as a simple reference point for the other models. The second running is the familiar one-loop result one gets by the method of the QCD β function [34, 35] and the third one is a phenomenological model trying to capture the significance of the dipole sizes during the scattering [33]. The motivation of this third model is that one usually expects in QCD that the hardest scale, i.e. now the smallest dipole, determines the running coupling in effect. Accordingly, the third model is called the smallest dipole prescription [33], and will be denoted as $\alpha_{s,min}$ in the figures of this chapter. The parameter C^2 of the third model used in [33] was set to $e^{-2\gamma_E}$ as was suggested in [36]. Additionally, the constant and one-loop couplings will be denoted by $\alpha_{s,C}$ and $\alpha_s(Q^2)$, respectively.

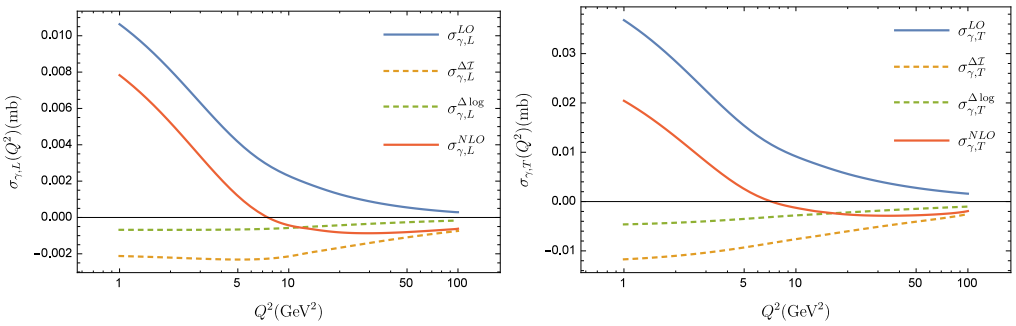

(a) Longitudinal. **(b)** Transverse.

Figure 4.1: Contributions of the two NLO terms shown separately for both longitudinally and transversly polarized cross section results. A constant α_s was used here.

With the polarized cross sections (4.1) we can also evaluate the DIS structure functions F_L and $F_2 \equiv F_L + F_T$:

$$F_{T,L}(q^+, Q^2) = \frac{Q^2}{(2\pi)^2 \alpha_{em}} \sigma^{\gamma}_{T,L}(q^+, Q^2). \tag{4.3}$$

The numerical evaluation of the cross section (4.1) was executed using Mathematica with the multidimensional integration library Cuba [37]. The Cuba library was used as the built-in numerical integration methods of Mathematica, both deterministic and Monte Carlo methods, proved incapable in the integration. Importance sampling of the integrand turned out to be crucial so the Monte Carlo methods 'Vegas' and 'Suave' of Cuba, that implement this, were suitable.

The cross sections were evaluated at a constant $q^+ \propto x^{-1} = x_0^{-1}$ with Q^2 varying between $1 - 100\,\mathrm{GeV}^2$. The fit parameters were set to the GBW results [32] so that $\sigma_0 = 23.03\,\mathrm{mb}$ and $Q_s(x_0) = Q_0 = 1\,\mathrm{GeV}$ at $x_0 = 3.04 \cdot 10^{-4}$. Results for the cross sections are shown in Fig. 4.2, where the calculated NLO contribution is compared to the LO result using the running coupling models (4.2). Results for the DIS structure functions are shown in Fig. 4.3 with a similar comparison.

The sensibility of the leading order results for the cross sections and structure functions shown in Figs. 4.2 and 4.3 were verified by a comparison with the cross section and DIS structure function results in [32]. The magnitude was found to be correct, although a one-to-one correspondence is not to be expected as the results in [32] are plotted with fixed invariant mass W slices, whereas here they are plotted

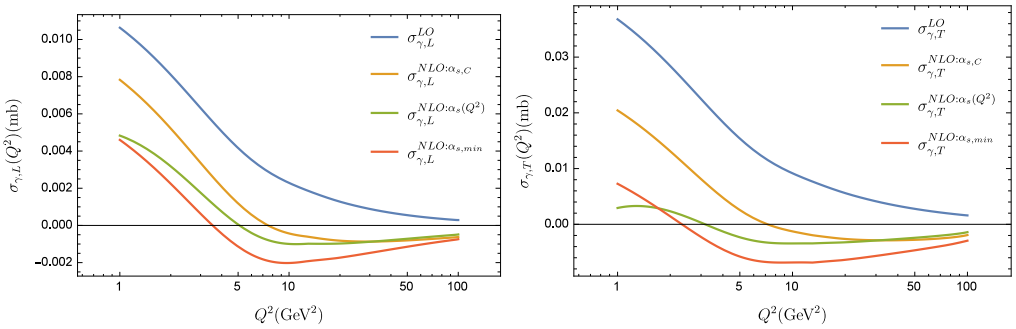

(a) Longitudinal. **(b)** Transverse.

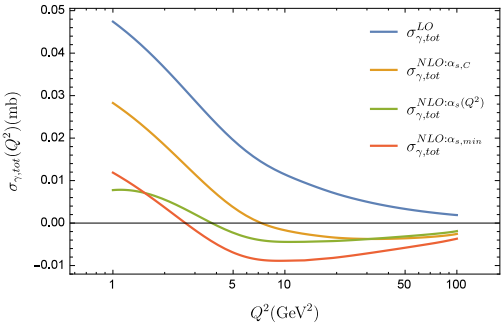

(c) Total cross section results.

Figure 4.2: Cross section results. Leading order results for longitudinal, transverse and total cross sections are shown with the computed NLO contributions with the three different QCD running coupling models.

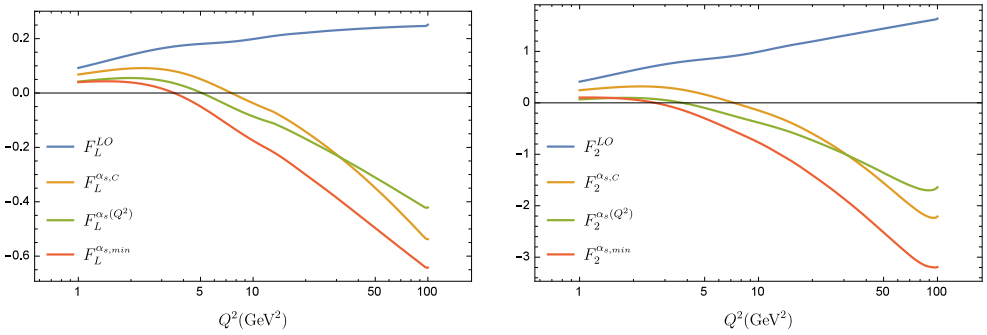

(a) **(b)**

Figure 4.3: Structure function results.

with a fixed x. This leads to the differing Q^2 dependence as $x = Q^2/(W^2 + Q^2)$.

Figures 4.1 and 4.2 demonstrate that the regularization did in fact work in making the NLO contributions finite. Past this, one immediately notices that the magnitudes of the computed NLO corrections are too large leading to large contributions to the LO results and even making the NLO cross sections, and thus the NLO structure functions, negative around $2 - 10\,\mathrm{GeV}^2$. This unphysical result was an expected shortcoming of the simple cut-off regularization implemented. A possible solution to a similar problem has been worked on in [38], where by implementing the factorization scale as dependent on the transverse momentum of the scattering product particle they are able to make the negative contribution at large momenta arbitrarily small. Fixing this problematic behavior is on the roadmap beyond this work.

From Figs. 4.1a and 4.1b one sees that for both of the polarizations the NLO contributions from both $\Delta\mathcal{I}^{NLO} = \Delta\mathcal{I}^{q\bar{q}g}$ and $\log(1 - z_1)$ terms are negative, the latter being somewhat smaller in magnitude. Interestingly neither of the contributions is strongly dependent on Q^2 in this region. Figures 4.2a and 4.2b show for both polarizations how the magnitude of the NLO contribution is strongly affected by the choice of the running coupling at low Q^2. For the transverse case the non-trivial running couplings lead to significantly smaller NLO cross sections in comparison to the LO cross section, meaning that the NLO contributions are unreasonably large in the whole Q^2 range. A similar conclusion follows for the longitudinal polarization result as well even if the effect is slightly less dramatic at low Q^2. Even though the magnitudes of the NLO cross section corrections decrease towards zero at high Q^2, this does not happen as quickly as the decrease of the LO result. This discrepancy is magnified in the structure function results shown in Fig. 4.3 where the NLO structure functions diverge from the LO result at $Q^2 \gtrsim 5\,\mathrm{GeV}^2$.

Chapter 5

Conclusions

The theoretical results derived in this work consist of partial next-to-leading order corrections to the polarized cross sections of virtual photon scattering from a classical color field. These were calculated using the light cone field theory starting from a parton Fock space expansion of the incoming photon state to get a perturbative result for the incoming virtual photon wavefunction. This calculation was done for the known leading order process $\gamma \to q\bar{q}$ and for the loopless NLO processes $\gamma \to gq\bar{q}$. Fourier transforming these wavefunctions into mixed space we got the results (3.9) along with (3.11) and (3.10) for the LO processes and (3.31) with (3.33) and (3.32) for the NLO processes. With these we were then able to use the eikonal approximation for the scattering process and the optical theorem to finally get the NLO cross sections (3.66), along with (3.14), (3.16), (3.62), and (3.63). Lastly it was necessary to regulate a soft divergence in the cross sections that was handled using a cut-off and subtracting the divergence into the dipole evolution prescription, yielding a convergent result (3.75). Lastly the result was rewritten using the impact parameter (4.1) to facilitate the numerical study.

The calculated NLO corrections are partial as in next-to-leading order there are non-trivial contributions to the quark-antiquark component of the photon splitting wavefunction due to several possible diagrams with internal gluon loops. Calculation of these diagrams is more involved than the quark-antiquark-gluon diagrams done here as they require more intricate regularization, and so were out of scope for this work. The NLO cross section result was written in a way that the loop

diagram contribution would be straightforward to include once is has been calculated.

In the numerical study done the derived next-to-leading order cross sections were evaluated and compared to established leading order results. The leading order results evaluated here were found to match earlier results. For the NLO contribution results the cut-off regularization used was found to be effective in eliminating the divergence. However, the regularization method is too crude and as a result the NLO contribution is over-subtracted into the evolution equation, causing the resulting next-to-leading order contributions become negative and large in magnitude. This in turn causes the next-to-leading order cross sections to become negative at high virtualities of the photon, which is unphysical. A more careful approach to the regularization is needed.

The full next-to-leading order result of the virtual photon scattering was out of scope for this work. To get the complete NLO result, two main tasks need to be done: firstly one needs to do the loop diagram calculations to get the full NLO wavefunction of the virtual photon and secondly it will be necessary to implement the dipole correlator solution via an evolution equation solver that takes NLO effects into account, a NLO BK equation solver for instance. With these issues resolved it should be possible to compare these theoretical results to experimental data to see if the agreement of the theory and data is improved at NLO with massless quarks.

Bibliography

[1] Nikolai Nikolaev and Bronislav G. Zakharov. Pomeron structure function and diffraction dissociation of virtual photons in perturbative QCD. *Z. Phys.*, C53: 331–346, 1992. doi:10.1007/BF01597573.

[2] Yuri V. Kovchegov and Eugene Levin. *Quantum chromodynamics at high energy*, volume 33. Cambridge University Press, 2012. ISBN 9780521112574, 9780521112574, 9781139557689. URL `http://www.cambridge.org/de/knowledge/isbn/item6803159`.

[3] Guillaume Beuf. NLO corrections for the dipole factorization of DIS structure functions at low x. *Phys. Rev.*, D85:034039, 2012. doi:10.1103/PhysRevD.85.034039.

[4] Edmond Iancu and Raju Venugopalan. The Color glass condensate and high-energy scattering in QCD. In *In *Hwa, R.C. (ed.) et al.: Quark gluon plasma* 249-3363*, 2003.

[5] Francois Gelis, Edmond Iancu, Jamal Jalilian-Marian, and Raju Venugopalan. The Color Glass Condensate. *Ann. Rev. Nucl. Part. Sci.*, 60:463–489, 2010. doi:10.1146/annurev.nucl.010909.083629.

[6] H. Kowalski, L. Motyka, and G. Watt. Exclusive diffractive processes at HERA within the dipole picture. *Phys. Rev.*, D74:074016, 2006. doi:10.1103/PhysRevD.74.074016.

[7] B. Z. Kopeliovich and B. G. Zakharov. Quantum effects and color transparency in charmonium photoproduction on nuclei. *Phys. Rev.*, D44:3466–3472, 1991. doi:10.1103/PhysRevD.44.3466.

[8] Stanley J. Brodsky, Hans-Christian Pauli, and Stephen S. Pinsky. Quantum chromodynamics and other field theories on the light cone. *Phys. Rept.*, 301: 299–486, 1998. doi:10.1016/S0370-1573(97)00089-6.

[9] Hans Gunter Dosch, T. Gousset, G. Kulzinger, and H. J. Pirner. Vector meson leptoproduction and nonperturbative gluon fluctuations in QCD. *Phys. Rev.*, D55:2602–2615, 1997. doi:10.1103/PhysRevD.55.2602.

[10] Guillaume Beuf. Dipole factorization for DIS at NLO I: Loop correction to the photon to quark-antiquark light-front wave-functions. *Phys. Rev.*, D94 (5):054016, 2016. doi:10.1103/PhysRevD.94.054016.

[11] I. Balitsky. Operator expansion for high-energy scattering. *Nucl. Phys.*, B463: 99–160, 1996. doi:10.1016/0550-3213(95)00638-9.

[12] Ian Balitsky and Giovanni A. Chirilli. Next-to-leading order evolution of color dipoles. *Phys. Rev.*, D77:014019, 2008. doi:10.1103/PhysRevD.77.014019.

[13] E. Iancu, A. H. Mueller, and D. N. Triantafyllopoulos. CGC factorization for forward particle production in proton-nucleus collisions at next-to-leading order. *JHEP*, 12:041, 2016. doi:10.1007/JHEP12(2016)041.

[14] Giovanni A. Chirilli, Bo-Wen Xiao, and Feng Yuan. Inclusive Hadron Productions in pA Collisions. *Phys. Rev.*, D86:054005, 2012. doi:10.1103/PhysRevD.86.054005.

[15] Kari Rummukainen and Heribert Weigert. Universal features of JIMWLK and BK evolution at small x. *Nucl. Phys.*, A739:183–226, 2004. doi:10.1016/j.nuclphysa.2004.03.219.

[16] Adrian Dumitru, Jamal Jalilian-Marian, Tuomas Lappi, Bjoern Schenke, and Raju Venugopalan. Renormalization group evolution of multi-gluon correlators in high energy QCD. *Phys. Lett.*, B706:219–224, 2011. doi:10.1016/j.physletb.2011.11.002.

[17] Yuri V. Kovchegov, Janne Kuokkanen, Kari Rummukainen, and Heribert Weigert. Subleading-N(c) corrections in non-linear small-x evolution. *Nucl. Phys.*, A823:47–82, 2009. doi:10.1016/j.nuclphysa.2009.03.006.

[18] M. Braun. Structure function of the nucleus in the perturbative QCD with N(c) —¿ infinity (BFKL pomeron fan diagrams). *Eur. Phys. J.*, C16:337–347, 2000. doi:10.1007/s100520050026.

[19] M. A. Kimber, J. Kwiecinski, and Alan D. Martin. Gluon shadowing in the low x region probed by the LHC. *Phys. Lett.*, B508:58–64, 2001. doi:10.1016/S0370-2693(01)00235-0.

[20] N. Armesto and M. A. Braun. Parton densities and dipole cross-sections at small x in large nuclei. *Eur. Phys. J.*, C20:517–522, 2001. doi:10.1007/s100520100685.

[21] E. Levin and M. Lublinsky. Parton densities and saturation scale from nonlinear evolution in DIS on nuclei. *Nucl. Phys.*, A696:833–850, 2001. doi:10.1016/S0375-9474(01)01132-0.

[22] M. Lublinsky. Scaling phenomena from nonlinear evolution in high-energy DIS. *Eur. Phys. J.*, C21:513–519, 2001. doi:10.1007/s100520100752.

[23] M. Lublinsky, E. Gotsman, E. Levin, and U. Maor. Nonlinear evolution and parton distributions at LHC and THERA energies. *Nucl. Phys.*, A696:851–869, 2001. doi:10.1016/S0375-9474(01)01150-2.

[24] E. Gotsman, E. Levin, M. Lublinsky, and U. Maor. Towards a new global QCD analysis: Low x DIS data from nonlinear evolution. *Eur. Phys. J.*, C27: 411–425, 2003. doi:10.1140/epjc/s2002-01109-y.

[25] Krzysztof J. Golec-Biernat, L. Motyka, and A. M. Stasto. Diffusion into infrared and unitarization of the BFKL pomeron. *Phys. Rev.*, D65:074037, 2002. doi:10.1103/PhysRevD.65.074037.

[26] Javier L. Albacete, Nestor Armesto, Alex Kovner, Carlos A. Salgado, and Urs Achim Wiedemann. Energy dependence of the Cronin effect from nonlinear QCD evolution. *Phys. Rev. Lett.*, 92:082001, 2004. doi:10.1103/PhysRevLett.92.082001.

[27] T. Lappi and H. Mäntysaari. Direct numerical solution of the coordinate space Balitsky-Kovchegov equation at next to leading order. *Phys. Rev.*, D91 (7):074016, 2015. doi:10.1103/PhysRevD.91.074016.

[28] T. Lappi and H. Mäntysaari. Next-to-leading order Balitsky-Kovchegov equation with resummation. *Phys. Rev.*, D93(9):094004, 2016. doi:10.1103/PhysRevD.93.094004.

[29] T. Lappi and H. Mäntysaari. Solving the NLO BK equation in coordinate space. *PoS*, DIS2015:080, 2015.

[30] T. Lappi and H. Mäntysaari. Solving the Balitsky-Kovchegov equation at next to leading order accuracy. In *Proceedings, 7th International Conference on Hard and Electromagnetic Probes of High-Energy Nuclear Collisions (Hard Probes 2015): Montréal, Québec, Canada, June 29-July 3, 2015*, 2016. doi:10.1016/j.nuclphysbps.2016.05.041. URL `https://inspirehep.net/record/1388020/files/arXiv:1508.03434.pdf`.

[31] T. Lappi and H. Mäntysaari. Balitsky-Kovchegov equation at next-to-leading order accuracy with a resummation of large logarithms. *PoS*, DIS2016:169, 2016.

[32] Krzysztof J. Golec-Biernat and M. Wusthoff. Saturation effects in deep inelastic scattering at low Q**2 and its implications on diffraction. *Phys. Rev.*, D59:014017, 1998. doi:10.1103/PhysRevD.59.014017.

[33] E. Iancu, J. D. Madrigal, A. H. Mueller, G. Soyez, and D. N. Triantafyllopoulos. Collinearly-improved BK evolution meets the HERA data. *Phys. Lett.*, B750:643–652, 2015. doi:10.1016/j.physletb.2015.09.071.

[34] G. M. Prosperi, M. Raciti, and C. Simolo. On the running coupling constant in QCD. *Prog. Part. Nucl. Phys.*, 58:387–438, 2007. doi:10.1016/j.ppnp.2006.09.001.

[35] Alexandre Deur, Stanley J. Brodsky, and Guy F. de Teramond. The QCD Running Coupling. *Prog. Part. Nucl. Phys.*, 90:1–74, 2016. doi:10.1016/j.ppnp.2016.04.003.

[36] T. Lappi and H. Mäntysaari. Single inclusive particle production at high energy from HERA data to proton-nucleus collisions. *Phys. Rev.*, D88:114020, 2013. doi:10.1103/PhysRevD.88.114020.

[37] T. Hahn. CUBA: A Library for multidimensional numerical integration. *Comput. Phys. Commun.*, 168:78–95, 2005. doi:10.1016/j.cpc.2005.01.010.

[38] B. Ducloué, T. Lappi, and Y. Zhu. Single inclusive forward hadron production at next-to-leading order. *Phys. Rev.*, D93(11):114016, 2016. doi:10.1103/PhysRevD.93.114016.